



University of
Stavanger

Faculty of Science and Technology

MASTER'S THESIS

Study program/ Specialization: Master in Offshore Engineering/ Environmental Technology	Spring semester, 2011 Open
Writer: Kathrine Woie (Writer's signature)
Faculty supervisor: Malcolm A. Kelland External supervisor(s): Anders Grinrød M-I SWACO, A Schlumberger Company	
Title of thesis: A study of the interaction between a kinetic hydrate inhibitor and selected corrosion inhibitors.	
Credits (ECTS): 30	
Key words: corrosion inhibitors, kinetic hydrate inhibitor, critical micelle concentration, LPR technique, hydrate RCS, compatibility	Pages:74..... + enclosure: Stavanger, Date/year

A study of the interaction between a kinetic hydrate inhibitor and selected corrosion inhibitors



**Master's Thesis
of
Kathrine Woie**

Faculty of Science and Technology
Department of Mathematics and Natural Science
Spring 2011



ACKNOWLEDGEMENT

This thesis was the final step in completing my master's degree in Environmental Technology at the University of Stavanger, Norway spring 2011. As the master program was mostly theoretical I wanted to do some practical work for my thesis. Anders Grinrød was my supervisor during my bachelor's thesis and I learned a lot. My wish was to carry out my master's thesis at M-I SWACO with Anders Grinrød being my supervisor.

Most of the laboratory work and writing process was carried out at M-I SWACO, A Schlumberger Company. Surface tension measurement was carried out in the laboratories at the University of Stavanger.

I would like to thank Anders Grinrød for giving me the opportunity to carry out my thesis at M-I SWACO. He took good care of me and made me feel like a part of his group.

Moreover I want to thank all employees at PT R&D and PT Technical Service for including me in lunch and other social events. A special thanks to Alexandra Cely for excellent guidance in the laboratory, but also giving me lots of work related input as well as private. This experience has been an excellent learning opportunity for me with lots of great people.

I also would like to thank Professor Malcolm A. Kelland for being my supervisor from the University of Stavanger and for the help he provided finishing my thesis. He also made an effort in creating a good dialogue between his students.

Finally I want to thank my husband Kenneth for supporting me through all these years of studying.

ABSTRACT

In field operations where natural gas hydrates can occur and CO₂ corrosion is a problem, chemicals called inhibitors can be employed. Kinetic hydrate inhibitors (KHIs) and corrosion inhibitors (CIs) are added in small concentrations to ensure flow assurance and for controlling CO₂ corrosion. When production chemicals are mixed fatal interactions can arise. Previous studies have been carried out and interactions have been revealed between different commercial KHIs and CIs. Finding a compatible CI/KHI package is of great interest for oil field companies in order to control two hazardous issues during petroleum production.

The purpose of this master's thesis was to study interactions between a commercial KHI and three different CIs. Surface tension measurements were performed prior to the corrosion and hydrate testing. Finding critical micelle concentration (CMC) for each solution containing both inhibitors was needed for selecting the proper CI concentration.

Two kinds of tests were performed for evaluating the chemical performance in the presence of one another. Corrosion testing was done in kettle tests by using the linear polarization technique. A hydrate rocking cell system was employed in the hydrate testing. CI efficiency and hydrate induction time was the parameters which were compared among the tests to reveal potential interactions.

Corrosion test results revealed a trend of antagonism between the KHI and two of the CIs. The third CI was slightly improved in the presence of the KHI. Hydrate test results revealed an antagonistic effect of CI to KHI performance. The hydrate induction time was reduced by more than 50 % in nearly all the test. One of the inhibitor combinations showed moderately compatibility in both tests.

Further research in this area could include a more detailed analysis of each couple to investigate what happens on a molecular level and at a surface. By understanding these mechanisms the search for a compatible CI/KHI package with certain qualities will be more efficient.

Table of Contents

ACKNOWLEDGEMENT	3
ABSTRACT	4
List of figures	7
List of tables	9
1 INTRODUCTION	10
2 LITERATURE REVEIW	11
2.1 Corrosion	11
2.1.1 CO ₂ corrosion.....	11
2.1.2 Corrosion control.....	13
2.1.3 Corrosion testing	15
2.2 Critical micelle concentration.....	16
2.2.1 Surface tension.....	17
2.3 Gas hydrates.....	19
2.3.1 Hydrate formation.....	21
2.3.2 Gas hydrate control.....	22
2.3.3 Chemical inhibitors.....	23
2.3.4 Hydrate testing.....	26
2.4 Compatibility studies.....	27
3 EXPERIMENTAL SETUP AND PROCEDURES.....	28
3.1 Surface tension measurements.....	28
3.1.1 Procedure	29
3.2 Corrosion testing	30
3.2.1 Equipment	31
3.2.2 Electrodes.....	33
3.2.3 Chemicals.....	33
3.2.4 Procedure	34
3.3 Hydrate testing.....	35
3.3.1 Equipment	35
3.3.2 Procedure	38
4 RESULTS AND DISCUSSION	39
4.1 Surface tension.....	39
4.1.1 Discussion.....	41
4.2 Corrosion Testing.....	42

4.2.1	Imidazoline A	43
4.2.2	Imidazoline B	47
4.2.3	Fatty Acid derivate.....	51
4.3	Hydrate testing.....	56
4.3.1	Luvicap 55W	57
4.3.2	Imidazoline A	58
4.3.3	Imidazoline B	59
4.3.4	Fatty Acid derivate.....	60
5	CONCLUSION	64
6	RECOMMENDATIONS.....	65
7	REFERENCES	66
8	LIST OF APPENDIX.....	68
	APPENDIX 1- STANDARD BUBBLE TEST (M-I SWACO)	69
	APPENDIX 2- HYDRATE PHASE ENVELOPE FOR GAS MIXTURE IN 0.1 % NACL.....	74

List of figures

Figure 1 CO ₂ corrosion affecting parameters [7]	12
Figure 2 Inhibition mechanism for a FFCI [6]	14
Figure 3 Experimental setup in LPR corrosion tests	15
Figure 4 Surface tension vs. concentration [16]	16
Figure 5 Kruss tensiometer (K6)	17
Figure 6 Stepwise process when using the DuNoüy-ring method [14].....	17
Figure 7 Structure of a typical methane hydrate [21]	19
Figure 8 Three different gas hydrate structures that can be formed [23]	20
Figure 9 Gas hydrate formation over time [18]	21
Figure 10 Agglomeration of hydrates in an oil – dominated system [25]	21
Figure 11 Hydrate equilibrium curve for a certain system [26]	22
Figure 12 A sub-cooling temperature chart [25]	23
Figure 13 Different KHIs and their chemical composition [25]	24
Figure 14 A conceptual diagram of the KHI mechanism [25].	25
Figure 15 Picture of the hydrate RCS rig from PSL.....	26
Figure 16 Sketch of a tensiometer by the DuNoüy -ring method [35].....	28
Figure 17 Setup of the Kettle test with a recirculation loop	31
Figure 18 Kettle test setup	32
Figure 19 Structure of VC/VP copolymer [36]	33
Figure 20 Parts in a hydrate test cell.....	35
Figure 21 Cells connected in the RCS	35
Figure 22 P-T diagram simulating the phase envelope of gas mixture G11 with 0.1% NaCl	37
Figure 23 Surface tension for Imidazoline A at different concentrations and 0.5 % Luvicap 55W	39
Figure 24 Surface tension for Imidazoline B at different concentrations and 0.5% Luvicap 55W	40
Figure 25 Surface tension for Fatty Acid der. at different concentrations and 0.5% Luvicap 55W ..	40
Figure 26 Performance of 10 ppm Imidazoline A	43
Figure 27 Percent efficiency of Imidazoline A.....	43
Figure 28 Performance of 30 ppm of Imidazoline A	44
Figure 29 Percent efficiency of Imidazoline A with and without the presence of Luvicap 55W	44
Figure 30 Performance of 80 ppm of Imidazoline A	45
Figure 31 Percent efficiency of Imidazoline A at 80 ppm	45
Figure 32 Average of the inhibitor efficiency.....	46
Figure 33 Performance of 10 ppm Imidazoline B	47
Figure 34 Percent inhibitor efficiency of 10 ppm Imidazoline B	47
Figure 35 Performance of 25 ppm Imidazoline B	48
Figure 36 Percent inhibitor efficiency of 25 ppm Imidazoline B	48
Figure 37 Performance of 50 ppm Imidazoline B	49
Figure 38 Percent inhibitor efficiency of 50 ppm Imidazoline B	49
Figure 39 Average efficiency of Imidazoline B	50
Figure 40 Performance of 5 ppm fatty acid derivate.....	51
Figure 41 Percent inhibitor efficiency of 5 ppm fatty acid derivate	51
Figure 42 Performance of 20 ppm fatty acid derivate.....	52
Figure 43 Percent inhibitor efficiency of 20 ppm fatty acid derivate	52
Figure 44 Performance of 5 ppm fatty acid derivate.....	53

Figure 45 Percent inhibitor efficiency of 70 ppm fatty acid derivate	53
Figure 46 Average performance of fatty acid derivate	54
Figure 47 Formed gas hydrate in one of the tests	56
Figure 48 Performance of 0.5 % Luvicap 55W tested in a hydrate RCS	57
Figure 49 Performance of Luvicap 55W in presence of 30 ppm Imidazoline A	58
Figure 50 Performance of Luvicap 55W in presence of 80 ppm Imidazoline A	58
Figure 51 Performance of Luvicap 55W in presence of 25 ppm Imidazoline B	59
Figure 52 Performance of Luvicap 55W in presence of 50 ppm Imidazoline	59
Figure 53 Performance of Luvicap 55W in presence of 20 ppm fatty acid derivate	60
Figure 54 Performance of Luvicap 55W in presence of 70 ppm fatty acid derivate	60
Figure 55 Induction time for each test with and without CIs in solution	61
Figure 56 Percent performance of Luvicap 55W in presence of CIs.....	62

List of tables

Table 1 Chemical structure of some typical FFCIs [10]	13
Table 2 Design matrix of the experiments	30
Table 3 Electrode composition	33
Table 4 Test conditions in corrosion testing	34
Table 5 Test concentrations in hydrate testing	36
Table 6 Gas composition	36
Table 7 Test conditions in hydrate testing.....	37
Table 8 Corrosion inhibitor concentration and surface tension values (± 1.0 mN/m).....	39
Table 9 CMC for each CI and selected test concentrations	41
Table 10 Average performance and standard deviation for the replicates.....	46
Table 11 Average performance and standard deviation for Imidazoline B replicates.....	50
Table 12 Average and standard deviation for fatty acid derivate	54
Table 13 Performance change of CIs in presence of Luvicap 55W	55
Table 14 Induction time for all test mixtures	61
Table 15 Summary of results	63
Table 16 Suggestion of test concentrations.....	65

1 INTRODUCTION

Well stream from the reservoir in oil and gas production is a complex mixture of liquid hydrocarbons (crude oil), produced water, hydrocarbon gas as well as CO₂ and H₂S gas.

CO₂ corrosion occurs when CO₂ reacts with water creating a weak acid in which reacts with iron in carbon steel constructions [1]. Gas hydrates can form during drilling, transportation, storage and gas processing plant [2]. To reduce corrosion and the prevention of hydrates in flow lines, production chemicals are added. If CO₂ corrosion and natural gas hydrates are allowed to form the outcome becomes hazardous. Flow assurance and corrosion rates are two parameters which are incredible important to control in petroleum production.

Although the chemicals perform great by its own compatibility problems can occur when different chemicals are mixed. Different studies have revealed interactions between CIs and KHIs. They have shown that KHIs can both enhance and depress CI performance while CIs totally depress KHI performance. Different theories have been suggested. CIs and KHIs are both surface active chemicals and adsorption competition can occur. Another theory is that they bond and depressing each other or enhancing their performance.

2 LITERATURE REVEIW

2.1 Corrosion

Corrosion was defined in 1946, by The American Electrochemical Society as “the destruction of a metal by chemical or electrochemical reaction with its environment”. Corrosion occurs due to the metals spontaneous need to revert to a more stable form as it is found in nature [3].

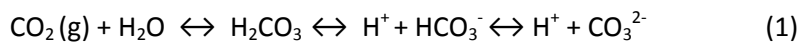
Four elements must be present for a corrosion cell to form [3-5]:

1. An electrolyte
2. A primary corrodent (O₂, CO₂, H₂S etc.)
3. A metal which have anodic and cathodic areas
4. Internal current path

Corrosion is a severe problem in the petroleum industry. As carbon steel is in contact with an aqueous phase, an electrolyte is generated and a corrosion issue arise. CO₂ corrosion also called sweet corrosion occurs due to CO₂ gas in the production fluids.

2.1.1 CO₂ corrosion

CO₂ is present as gas in formation fluids and in solution in oil and water. When CO₂ gas is in contact with water following reactions takes place [3]:



The pH in solution decreases as carbon dioxide slowly forms carbonic acid and bicarbonate. This pH reduction creates an electrolyte where iron (Fe²⁺) dissolves into solution. Some reacts with the bicarbonate to create a deposit on the steel, iron carbonate (FeCO₃) as shown in equation 2 [3, 6].



Corrosion reactions and the corrosion rate is affected by environmental, physical and metallurgical parameters [7]. These parameters are categorized in figure 1.

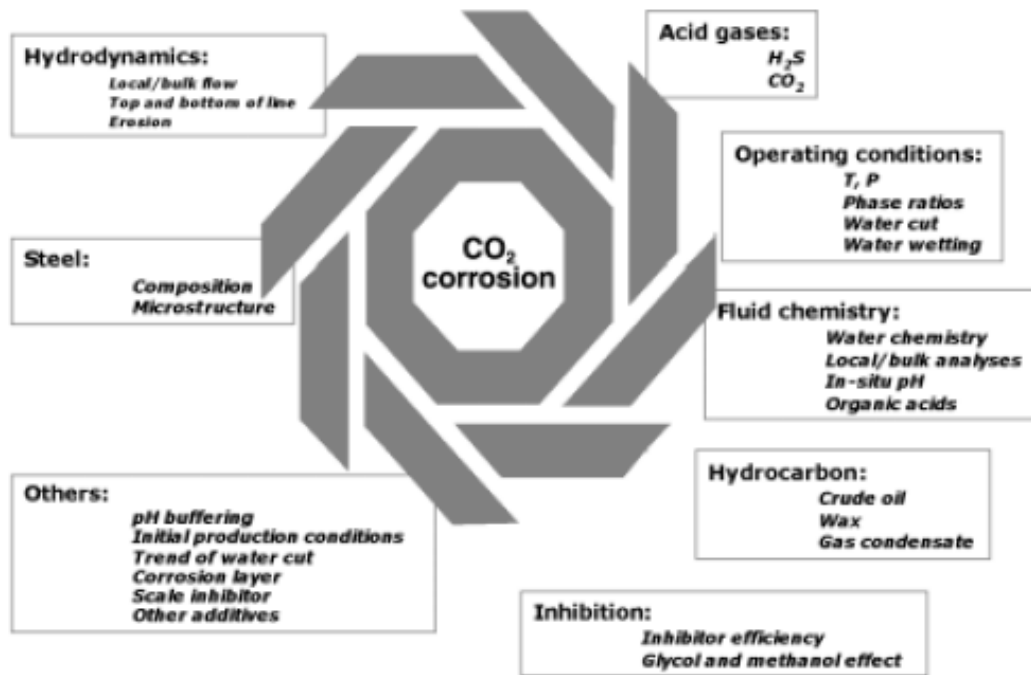


Figure 1 CO₂ corrosion affecting parameters [7]

CO₂ content in solution is temperature and pressure determinant. As pressure increases or temperature is decreasing, more CO₂ can dissolve.

2.1.2 Corrosion control

Corrosion control is achieved in different ways but the main purpose is to block one or more of the elements that is essential for a corrosion cell [5]. Chemical treatment is a common inhibition method employed in petroleum production.

2.1.2.1 Corrosion inhibitors

To reduce the corrosion rate CIs can be added. It is a chemical substance that has the ability to decrease corrosion rate. Inhibition can be grouped based on functional behaviour [3, 5].

- Adsorption of an invisible film that protect the metal surface.
- Chemical reaction between the inhibitor and the metal or the environment.
- Precipitation reaction causing a precipitate that covers the metal surface as a protective layer.

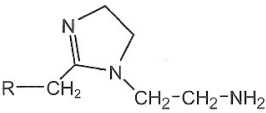
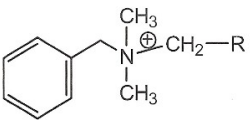
CO₂ corrosion in oil, condensate and gas protection lines is mainly decreased by using film forming corrosion inhibitors (FFCIs) that are organic compounds. They usually contains nitrogen and a long hydrocarbon tail (C₁₈) [5, 8].

Fink classify them in following groups [9]:

- Amides and Imidazolines
- Salts of nitrogenous molecules with carboxylic acids (fatty acids, naphthenic acids)
- Nitrogen quaternaries
- Polyoxylated amines, amides, and Imidazolines
- Nitrogen heterocyclics

Chemical structure on some typical FFCIs is summarized in table 1.

Table 1 Chemical structure of some typical FFCIs [10]

Chemical name	Structure
Primary amine	$R-CH_2-NH_2$
Amide	$R_1-CH_2-C(=O)-NH-R_2$
Imidazoline	
Quaternary ammonium ion	
Polyethoxylated amines	$R-N \begin{cases} (O-CH_2-CH_2)_n OH \\ (O-CH_2-CH_2)_n OH \end{cases}$

FFCIs have surface active properties as surfactants [5]. Surfactants are a chemical class of components that consist of a hydrophobic tail and a hydrophilic head. The hydrophobic tail is oil-loving and the hydrophilic head is water-loving. They adsorb to the metal surface which will generate an oil barrier between the produced fluids and the metal [6]. Figure 2 show the barrier that is developed when a FFCI is protecting the metal.

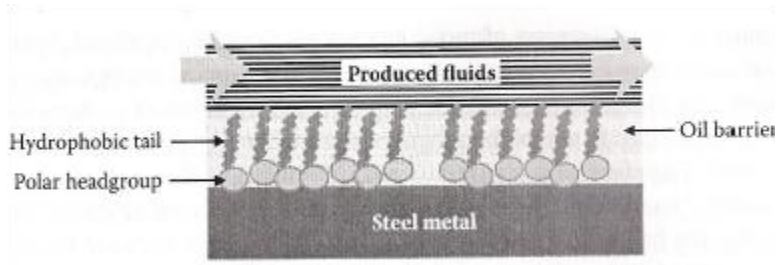


Figure 2 Inhibition mechanism for a FFCI [6]

Smaller molecules and polymers can also adsorb to a metal surface creating a protective “film”. This “film” is made by the inhibitor alone or by binding with the metal resulting in a complex. They are on the other hand not forming the extra barrier that a surfactant does due to its hydrophobic tail [6].

2.1.3 Corrosion testing

CI performance can be evaluated by different test methods such as bubble/kettle test, flow loop test, rotating cylinder electrode (RCE) test and high shear autoclave among others [6]. The kettle test was used in this study. This test is easy to carry out and it is possible to produce a large amount of data in a short period of time.

A kettle is filled with fluids that act as an electrolyte and inhibitor performance is evaluated by linear polarization resistance (LPR) technique. An electrochemical resistance is measured between two electrodes of metal inserted into solution. One electrode works as an anode and the other as a cathode. By applying a small voltage which is not interfering with the actual corrosion process, the resulting current flow is measured. As the system is exposed to a corrosive gas and metal is corroding, the resistance between the electrodes is getting smaller which corresponds to higher corrosion rate which is shown from the equation 3 [11].

$$R = \frac{V}{I} \quad (3)$$

Polarization resistance (R) is the ratio between the applied voltage (V) and the measured electrical current (I) and is inversely proportional to the corrosion rate.

The system is saturated with CO₂ to remove oxygen from the system to simulating pipeline conditions. CO₂ is reacting with water to form the weak acid H₂CO₃ that react with iron at the metal surface; a corrosion cell is established. The metal coupons are allowed to corrode for a period of time before the inhibitor is added and the inhibitor performance is evaluated. A good CI should be able to depress corrosion rate to 0.1 mm/year and keep it there for at least 24 hours.

Figure 3 show the experimental setup of the kettle testing that was performed in this study.

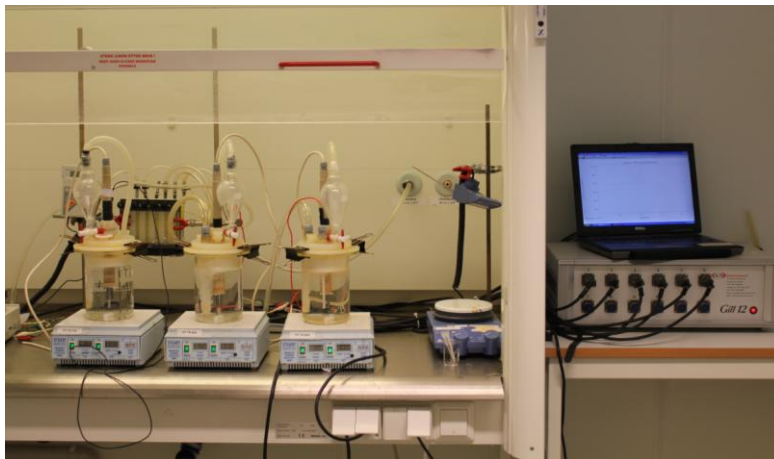


Figure 3 Experimental setup in LPR corrosion tests

The efficiency of an inhibitor is calculated by using equation 4 [4]:

$$\% \text{ inhibition efficiency: } \left(\frac{R_0 - R_1}{R_0} \right) \times 100\% \quad (4)$$

Where R₀ = corrosion rate without inhibitor, R₁ = corrosion rate with inhibitor at 15 hours.

2.2 Critical micelle concentration

When surfactants are added to a water solution they will orient themselves so that hydrophilic head faces towards the water and the hydrophobic tail is at the liquid surface. As the number of surfactants increases and the surface is being covered with surfactants, the liquid surface tension is lowered. As the amount of surfactants reaches a maximum and covers the whole surface, the excess of surfactants will start forming micelles in solution. This point is known as the critical micelle concentration (CMC) [12-15]. At this point the surface tension is constant regardless of increasing surfactant concentration. This is shown in figure 4.

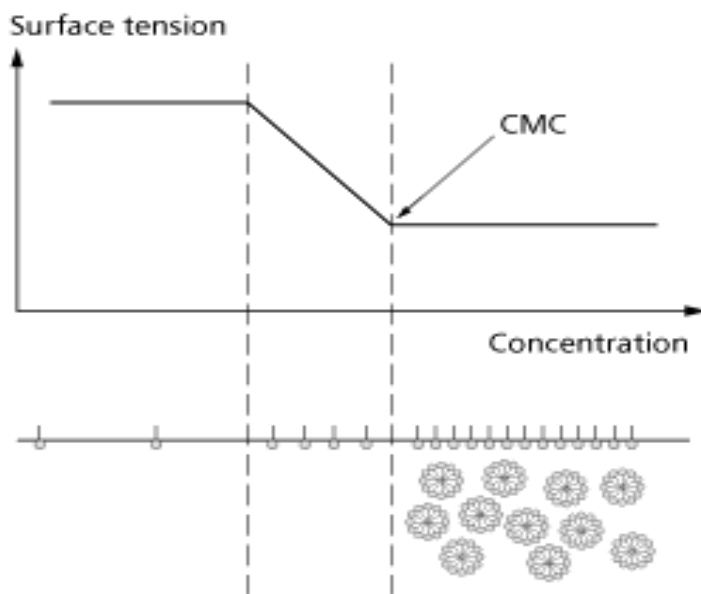


Figure 4 Surface tension vs. concentration [16]

2.2.1 Surface tension

Surface tension for a surfactant solution can be measured with a tensiometer by different methodologies. In this thesis DuNoüy- ring method was employed with a Krüss tensiometer (K6) as is shown in figure 5.

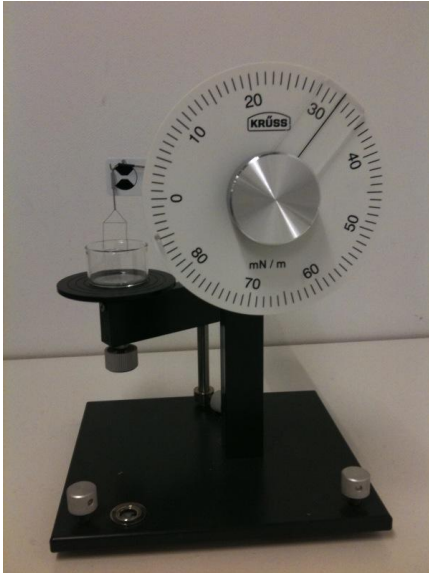


Figure 5 Krüss tensiometer (K6)

A platinum ring is inserted in the interface of a solution. The ring is raised with an applied force and a meniscus of solution is formed. When enough force is added the meniscus will eventually break and the surface tension is determined. This process is shown in figure 6.

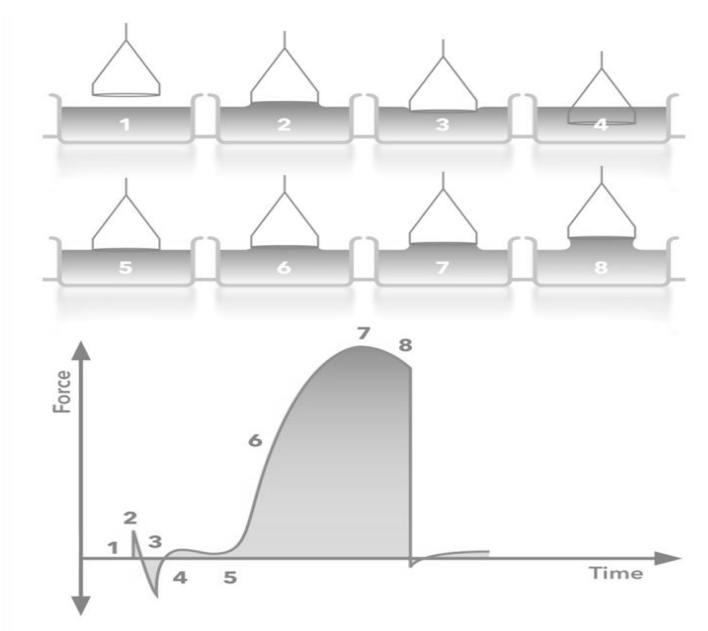


Figure 6 Stepwise process when using the DuNoüy-ring method [14]

Step 1-4 represents the process where the ring is inserted in the interface of the solution. At step 5 the ring is raised to the point where the meniscus forms. In step 8 after the maximum force is applied there will be a small decrease of force needed, before the lamella will break.

DuNoüy-ring method is an easy and fast method used to measure surface tension and for finding CMC for a surfactant solution [17].

The CMC for a surfactant in solution is important to know in order to add a chemical in the right concentration. There must be sufficient chemical to ensure maximum protection but over dosage must be prevented due to chemical performance, economics and compatibility.

2.3 Gas hydrates

The discovery of a solid composed of water and gas formed above freezing point for pure water was documented by Sir Humphrey Davy in 1810 [18].

Natural gas hydrate is a crystalline solid that is composed of water and natural gas. It looks like ice crystals but has different properties. It forms above 0° C and is flammable in comparison to ice. When a well stream reaches a critical temperature level, water molecules arrange in a lattice by hydrogen bonding. Different cavities are formed which are able to trap certain gas molecules (<0.9 nm). The gas molecules can be methane (CH₄), ethane (C₂H₆), propane (C₃H₈), isobutene (iso-C₄H₁₀) and carbon dioxide (CO₂). This bonding contributes to the stabilization of the hydrate structure by van der Waal forces [6, 18-20].

Three conditions are required for a hydrate to form [19]:

1. Critical temperature and pressure. Hydrates are formed at low temperatures and high pressures.
2. Water needs to be present.
3. Proper gas molecules must be available in the system.

Figure 7 shows the structure of a gas hydrate with methane (CH₄) trapped in the cavities.

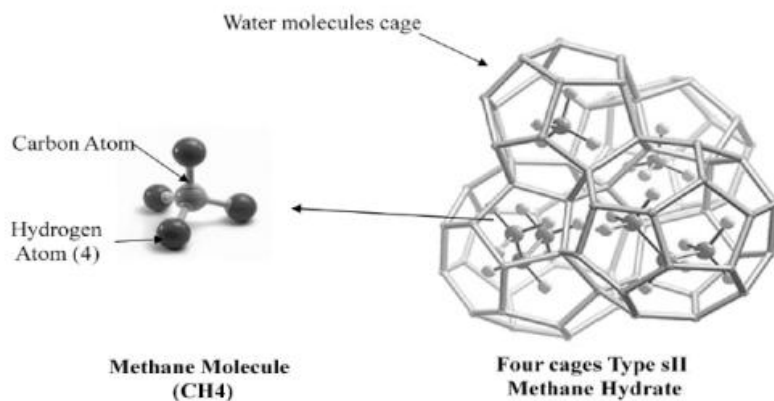


Figure 7 Structure of a typical methane hydrate [21]

Gas hydrates exist as three different structures; structure I (sI), structure II (sII) and structure H (sH). They differ by the crystal structure and the water/gas ratio. If the natural gas contains a lot of methane (CH₄), sI is most likely to form. sII is primarily formed in petroleum production due to the gas composition including butane and propane beside methane. sH is stabilized when both a small and a large gas molecule occupy cavities at the same time [6, 18, 22].

Figure 8 show the structure of sI, sII and sH gas hydrates.

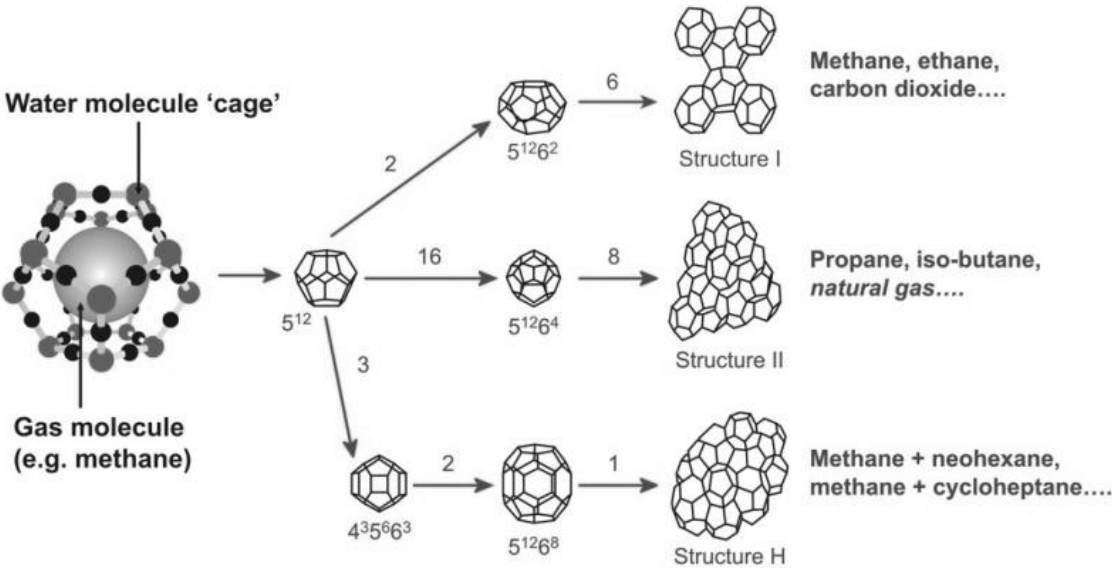


Figure 8 Three different gas hydrate structures that can be formed [23]

Usually one cage contain only one guest molecule. As all the cages are filled, the composition of the hydrate is similar for all different structures; 15 mol% guest(s) and 85 mol% water [22].

2.3.1 Hydrate formation

Hydrate formation occurs in two major steps; hydrate nucleation and hydrate growth. The hydrate nucleation occurs very fast. This growth process is stochastic. Figure 9 show the hydrate formation curve in a system operated in constant temperature and pressure.

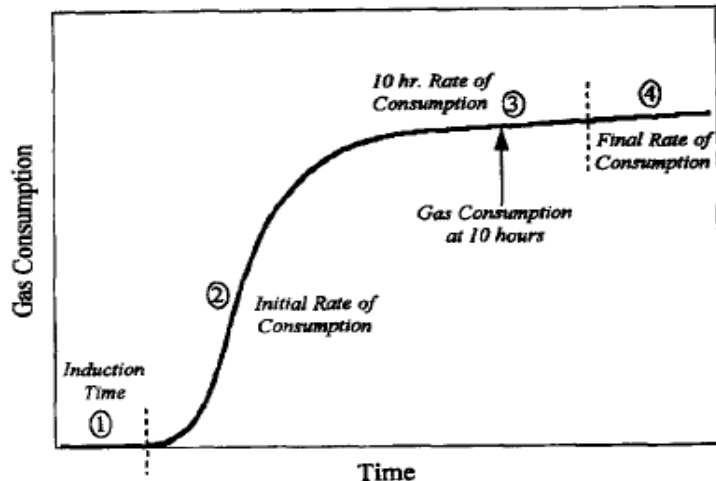


Figure 9 Gas hydrate formation over time [18]

The induction time (1) is defined by Sloan [18] as “the time elapsed until the appearance of a detectable volume of hydrate phase or, equivalently, until the consumption of a detectable number of moles of hydrate former gas”. This period is represented in practical experiments when the liquid turns cloudy. In field operations this induction time is the most critical factor [24]. The growth period (2) is when gas is being trapped in the hydrate cages. In this period the hydrate growth rate is catastrophic. The periods (3-4) are where stabilization occurs due to the minimal amount of water left.

Sloan et al. divide flow line systems into four models based on the production composition. Oil-dominated systems, gas-dominated systems, gas condensate systems and high water cut (volume) systems. A conceptual figure that shows the forming of a hydrate plug in an oil-dominated system is represented in figure 10. In this system the water cuts are low (<50Vol %).

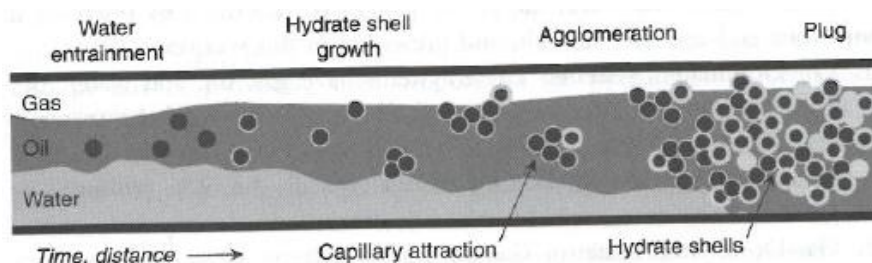


Figure 10 Agglomeration of hydrates in an oil – dominated system [25]

Three phases can be seen in the figure; gas on top, oil in the middle and water as the heaviest component at the bottom. Although water is present in its own phase, water droplets can be dispersed into the oil phase. Water-in-oil emulsions are formed. When the critical temperature and pressure is reached the flow line is entering the hydrate formation region. Hydrates will start growing on the droplets rapidly and a hydrate shell is formed. As the number of hydrate droplets increases a hydrate plug will eventually form [25].

2.3.2 Gas hydrate control

To avoid gas hydrates in pipelines the critical hydrate formation pressure and temperature has to be known. Hydrate equilibrium properties are found experimentally and plotted in a pressure-temperature diagram. Figure 11 show a hydrate equilibrium curve for a given system. To prevent hydrate formation, pressure and temperature needs to be operated in the hydrate free zone which is to the right for the equilibrium curve.

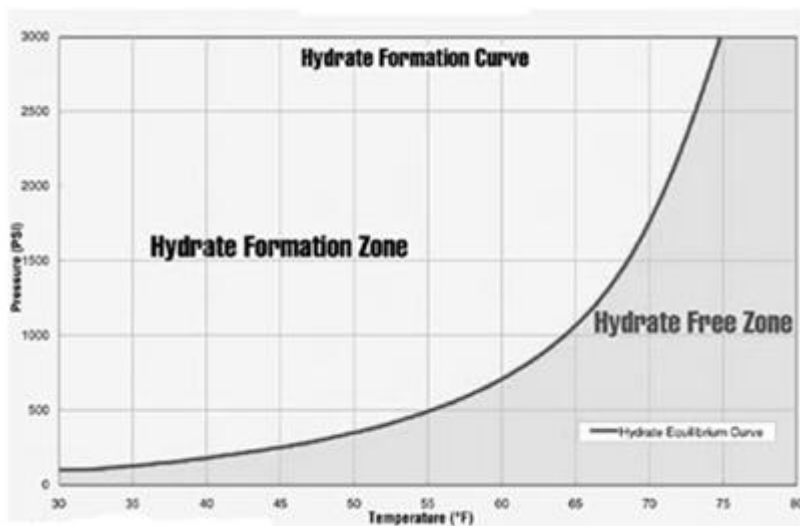


Figure 11 Hydrate equilibrium curve for a certain system [26]

The driving force in hydrate formation is sub-cooling (ΔT). Sub-cooling is the difference between the operating temperature and the temperature which hydrates are formed at constant operating pressure. If the pressure is somehow constant in the production line while the temperature is dropping, the system will move into the hydrate formation area [6, 25]. Inhibitors are ranked according to sub-cooling performance and induction time. Figure 12 show another pressure-temperature graph which display the sub-cooling rate.

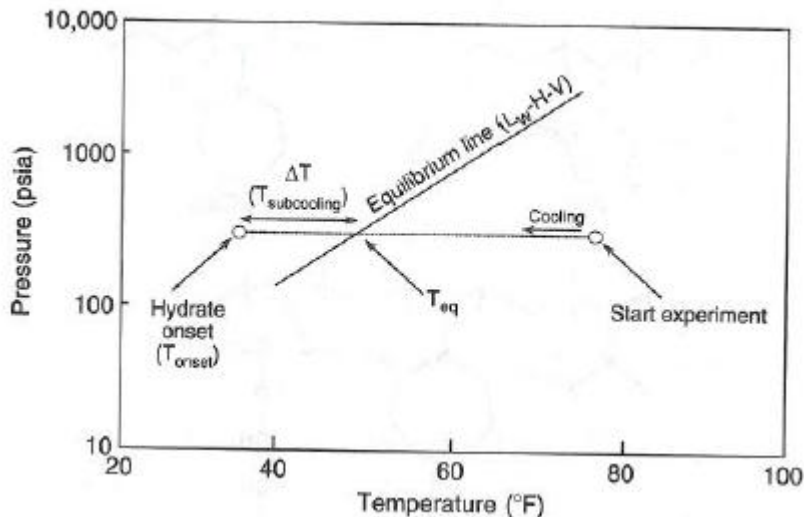


Figure 12 A sub-cooling temperature chart [25]

The equilibrium line in figure 12 separates the areas where hydrate formation occur (left) and the hydrate free zone (right). As the temperature decreases, at a constant pressure, the fluid will eventually reach the equilibrium temperature (T_{eq}). As the temperature is decreased further the onset temperature (T_{onset}) for hydrate formation will be reached and hydrates are formed [25].

2.3.3 Chemical inhibitors

Hydrate formation can be controlled in different ways by removing one of the factors favoring gas hydrate formation. Chemicals known as hydrate inhibitors can be employed to decrease the hydrate formation. They are classified in two different classes; thermodynamic inhibitors (THIs) and low dosage hydrate inhibitors (LDHIs).

2.3.3.1 Thermodynamic inhibitors

THIs includes alcohols (methanol or ethanol) and glycols (mono- ethanol glycol or di-ethylene glycol) and is required in a large amount. The concentration can be as high as 60 wt% based on the water phase. When THI is added the thermodynamic properties of the solution is changed so that lower temperature and higher pressure is needed to before hydrates are formed. THIs can also be used to “melt” existing hydrates [6].

Large costs are related to the use of THIs. High volumes and expensive storage and the need for regeneration facilities are some examples. Other operational factors such as toxicity, flammability and pollution of the hydrocarbon phase among others matters in choosing the right inhibitors. During the nineties new classes of chemical inhibitors were developed; The LDHIs [6].

2.3.3.2 LDHIs

LDHIs are grouped in two classes; KHIs and anti- agglomerants (AAs). They inhibit hydrate formation by different mechanisms. KHIs interfere directly in the formation of the hydrate crystals (kinetics) while AAs bonds to the hydrate crystals and prevent the agglomeration and keep them dispersed in the hydrocarbon phase. As the name implies the required concentration of LDHIs is low. In field operations normally 0.1-1 wt% (active) is needed based on the water phase [24]. A KHI can give a 10°C depression of hydrate onset temperature at a dose of 0.5 wt% whereas 20 wt% methanol is required for the same depression [4].

The performances of KHIs and AAs are affected by the composition of the hydrocarbon phase, salinity and other additives. Physical parameters like pressure and mixing can also affect inhibitor performance [24].

2.3.3.3 KHIs

Chemicals that work as KHIs are small polymers with a low molecular weight. In all known KHIs the key components are [6]:

- Polymers containing functional pendant groups. Usually these groups are amide groups that can bond to water molecules or hydrate particles.
- A hydrophobic group that can bond adjacent or directly to the amide group.

Figure 13 show the chemical composition of some KHIs.

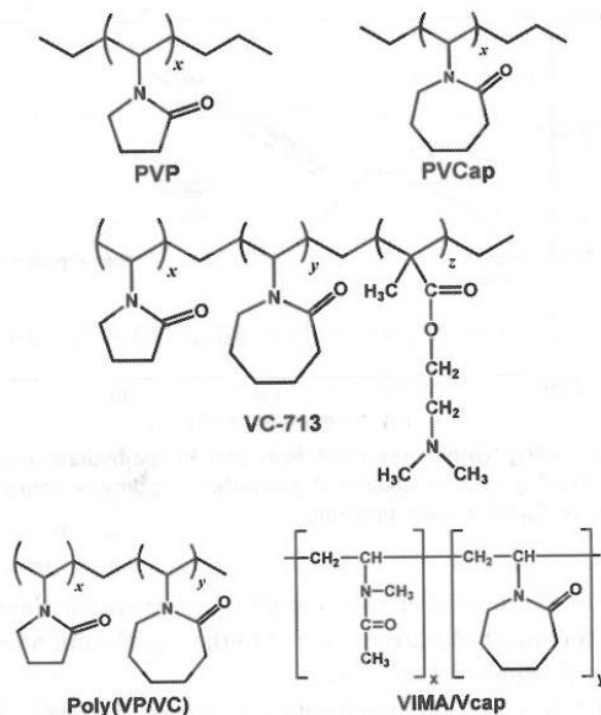


Figure 13 Different KHIs and their chemical composition [25]

Most KHIs are polar molecules and they perform in the water phase. KHIs slow down the hydrate growth by binding to the surface. It is the pendant amide group that enters and blocks some of the cages on the hydrate crystal structure and the polymer is anchored to the surface [18, 25].

KHI performance is evaluated by its sub-cooling rate and the ability to delay induction time. In general, the higher sub-cooling the lower is the induction time. KHIs can only depress hydrate growing in a fluid for a certain time period so its performance is time dependent [6, 25].

The sub-cooling is increased when the polymer KHIs are adsorbed more closely at the crystal surface and depress further crystal growth. This is visualized in figure 14.

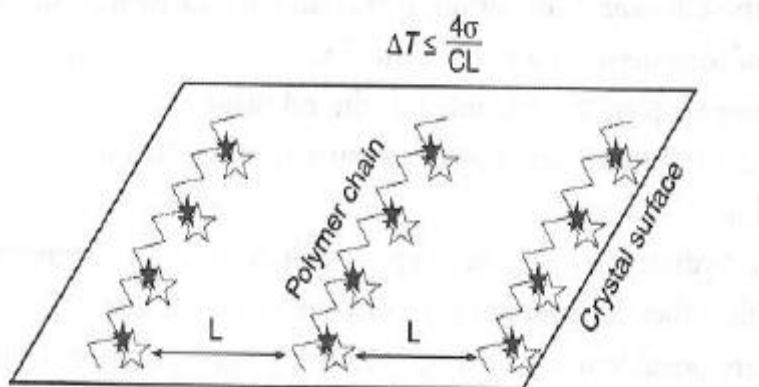


Figure 14 A conceptual diagram of the KHI mechanism [25]

KHI performance and the degree of sub-cooling can be related by equation 5 [25].

$$\Delta T = 4\sigma/CL \quad (5)$$

Where ΔT is sub-cooling, σ is the surface energy, C is a constant and L is the length between the polymer chains.

In field applications sub-cooling are limited to a maximum of 9-10°C for most of the commercial KHIs [6].

2.3.3.4 AAs

AAs are on the contrary to KHIs long molecules and can be either a surfactant or a polymer [25, 27]. AAs don't disrupt the crystal growing but are converting all emulsified water in the oil phase to hydrates. The hydrophilic part of the AA attaches to the hydrate particle while the hydrophobic tail keep them in suspension with the oil [25]. AA performance depends upon three factors: hydrocarbon composition, brine concentration and the water cut [28]. AAs perform at higher sub-cooling than KHIs so they can be used in deepwater applications where temperature is lower [24].

The drawback for AAs compared to KHIs regards the environmental aspect. Most AAs are toxic for marine species and have low biodegradation.

2.3.4 Hydrate testing

Hydrate testing can be carried out in autoclaves, rocking cells, pipe wheels and loops. In this study the KHI performance was evaluated in a hydrate rocking cell system (RCS) from PSL. Small sapphire cells containing a steel ball are placed in a water bath. Since the cells are made of sapphire glass, it is possible to see when hydrates are formed. The cells are pressurized and rocked as the temperature is slowly decreased at a constant pressure. When the ball stops moving it indicates that the cells are plugged with hydrates. Pressure, temperature and run-time sensors are connected to each cell. Software is recording and processing the recorded information. Pipeline conditions can be simulated due to various settings which can be changed in the software that comes with the rig. Pressure, temperature and run-time graphs can be evaluated during and after the experiment. Figure 15 shows the RCS rig and the cooling unit.

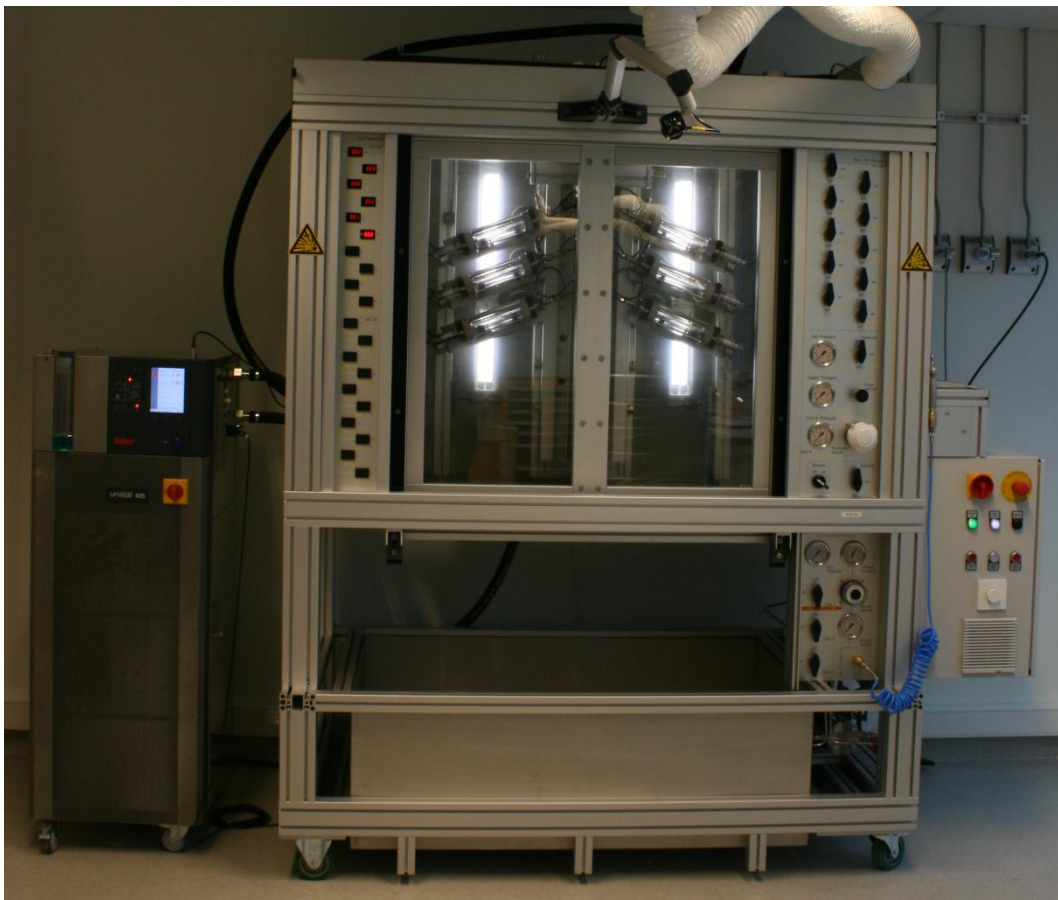


Figure 15 Picture of the hydrate RCS rig from PSL

A decrease in gas consumption implies that gas hydrate formation is occurring [29]

2.4 Compatibility studies

When production chemicals are mixed their performance can change due to interactions. Such changes must be avoided in all circumstances. It is important to do compatibility studies when testing new chemicals in both small and large scale.

Studies have revealed interaction between CIs and KHIs. CIs have the tendency to depress KHI performance. During the same studies KHIs have showed neutral, negative and positive effects to CI performance. Some theories have been proposed: competition between CI and KHI due to their surface active properties, direct interaction between them resulting in a better or worse adsorption property [2, 6, 20, 30-32].

Other studies have shown that surfactants have a strong influence on the kinetics in hydrate formation. This accelerating of hydrate formation is caused by their inherent foaming properties and their ability to form micelles [33, 34].

3 EXPERIMENTAL SETUP AND PROCEDURES

The purpose of these experiments was to study the interaction between a KHI (Luvicap 55W) and three different CIs. CI performance was measured with and without the presence of a KHI, using LPR technique in a kettle test. Hydrate induction time was compared in a RCS for a KHI with and without the presence of three different CIs. KHI concentration was constant in all of the tests. Three concentrations were selected for each CI on the basis of surface tension measurements.

3.1 Surface tension measurements

The purpose of finding the CMC for the solution was to use this concentration further in corrosion and hydrate testing. The solution was made of 0.1 wt% NaCl, 5000 ppm Luvicap 55W and CI added in different concentrations ranging from 5 ppm to 500 ppm. 40 ml solution was made in glass vials and the surface tension measurements took place after 24 hours. Surface tension was measured with a Kruss tensiometer (figure 16).

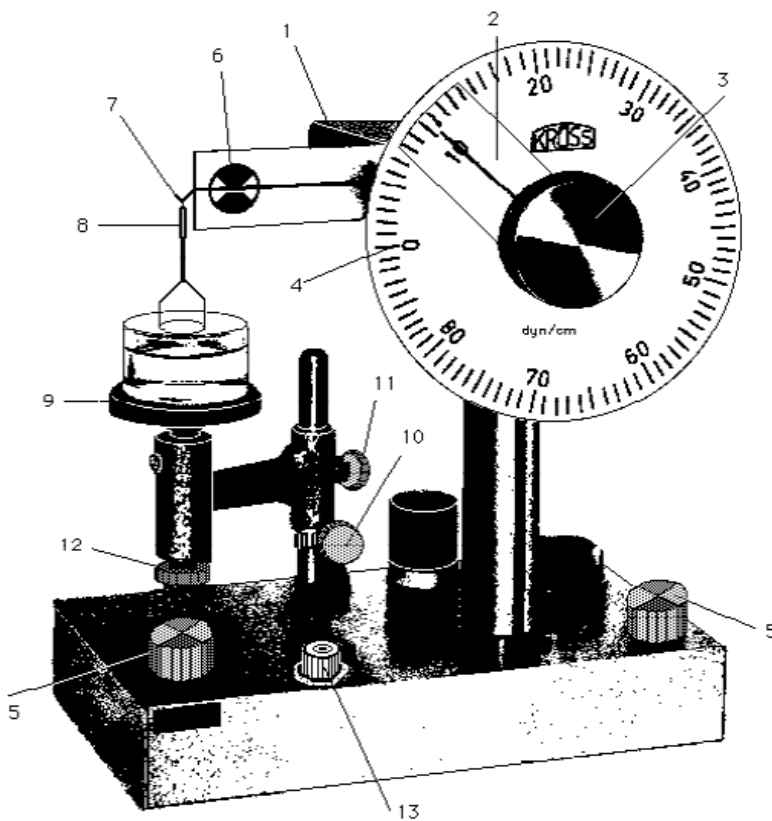


Figure 16 Sketch of a tensiometer by the DuNoüy -ring method [35]

3.1.1 Procedure

The procedure for using the tensiometer is described in 8 steps found in a laboratory course in biophysical chemistry [35].

1. The instrument needs to be placed on a stable horizontal position and 13 indicate if it is horizontal. If this needs to be adjusted the two knobs (5) can be used.
2. Table (9) is raised up by using the screws (10 and 11) so the glass container with the test liquid was underneath the ring.
3. The ring is made of platinum and must be handled careful to avoid deformation. It should be heated until it glows red in a flame prior each measurement.
4. Approximate 20 ml of solution was filled in the glass container. The container is placed in the middle of the holder (9) and in the centre.
5. Prior the measurement the table is adjusted up by the screw (12) to the maximum. This screw is used also in the measurement.
6. The pointer (3) needs to adjust so it points at zero. Mark (6) is a level indicator and the wire should always be within the white area.
7. The ring is in solution when the measurement starts. The big wheel (3) is adjusted a bit to the left so the ring is pulled in.
8. The wire (6) is then raised up into the black area and it needs to be adjusted with the screw (12). This is done carefully until the ring breaks with the surface. The surface tension (mN/m) is then read off and a new measurement can take place with just repeating step 3-8.

The recorded values were rounded to the nearest whole number so the data has an error of ± 0.1 mN/ m.

Calibration of the instrument was done by measuring surface tension in double distilled water at 20°C which has the surface tension 72.75 mN/m. If another value was obtained, the recorded values had to be corrected with that factor to achieve correct results.

3.2 Corrosion testing

The standard Bubble/kettle test was performed according to the M-I SWACO test standard (Appendix 1) which is based on reference ASTM G59 (“Practise for Conductivity, Potentiodynamic Polarization Resistance Measurements”).

The corrosion rate for mild steel was examined by kettle test. Three replicates were performed for each concentration for each corrosion inhibitor. The concentrations were randomly selected after finding the CMC each CI/KHI solution (chapter 4). One concentration above, one below and the actual critical micelle concentration (CMC) was examined. The experimental design is shown in table 2.

Table 2 Design matrix of the experiments

Imidazoline A	Experiments
10 ppm+0.5%HI	3
30 ppm+0.5%HI	3
80 ppm+0.5%HI	3
10 ppm, No HI	3
30 ppm, No HI	3
80 ppm, No HI	3
Imidazoline B	
10 ppm+0.5%HI	3
25 ppm+0.5%HI	3
50 ppm+0.5%HI	3
10 ppm, No HI	3
25 ppm, No HI	3
50 ppm, No HI	3
Fatty Acid derivate	
5 ppm+0.5%HI	3
20 ppm+0.5%HI	3
70 ppm+0.5%HI	3
5 ppm, No HI	3
20 ppm, No HI	3
70 ppm, No HI	3

3.2.1 Equipment

Bubble test apparatus includes:

- Hot plate/Stirrer,
- Magnetic stirring bar,
- Glass Wessel's, lids and stopper.
- Metal clamps for lids
- Gas sparge tubes linked to CO₂ supply,
- Probes attached to ACM instruments PC monitoring system
- PC for logging
- Micropipette
- Test brine (0.1% NaCl)
- Distilled water
- Acetone
- Electrodes (C1018)
- Cls
- 5000 ppm Luvicap 55W
- 10 % Hydrochloric acid solution for cleaning
- Scientific CO₂ (g)
- Recirculation loop if foaming problems (separating funnel and a flexible tube)

Foam was formed when hydrate inhibitor was combined with Imidazoline A and Imidazoline B. A recirculation loop made of separation funnel which was added in the setup in order to decrease the foam loss (figure 17).

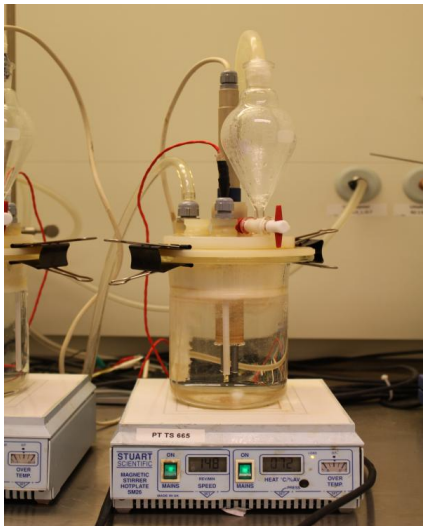


Figure 17 Setup of the Kettle test with a recirculation loop

Normally a defoamer would have been added in field testing to depress foaming. But as the surface tension was measured in a system with just corrosion inhibitor and hydrate inhibitor this was left out.

The test setup coupled to the ACM instrument and monitoring system is in figure 18.

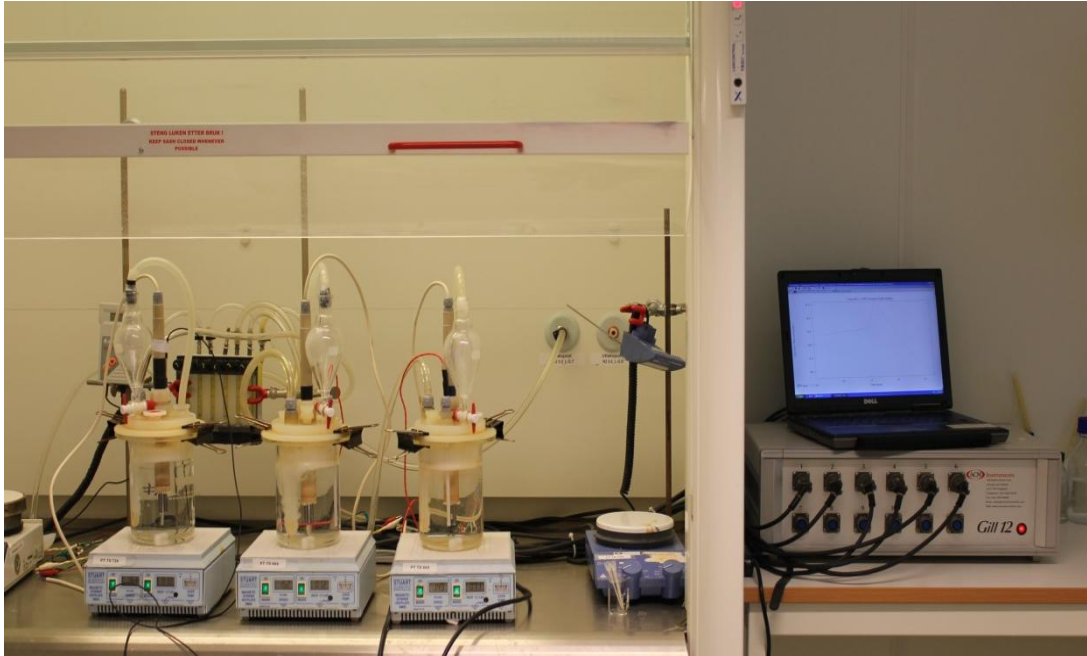


Figure 18 Kettle test setup

3.2.2 Electrodes

The electrodes were made of mild steel with area 4.897 cm². Steel composition is represented in table 3.

Table 3 Electrode composition

Element	Conc. (%)	Element	Conc. (%)
Al	0,03	Mn	0,85
C	0,18	Mo	0,02
Cr	0,02	Nb	0,01
Cu	0,02	Ni	0,03
P	0,02	S	0,02
Si	0,24	Sn	0,004
Ti	Trace	Fe	98,58

3.2.3 Chemicals

Three available CIs were chosen randomly; two different Imidazoline's and a fatty acid derivative. They were named Imidazoline A, Imidazoline B and fatty acid derivative.

A commercial KHI, Luvicap 55W were chosen as the hydrate inhibitor. Luvicap 55W is a copolymer with a low molecular weight. Its active component is a 1:1 mixture of two small polymers called vinyl caprolactam (VC) and vinyl pyrrolidone (VP) copolymer (figure 19).

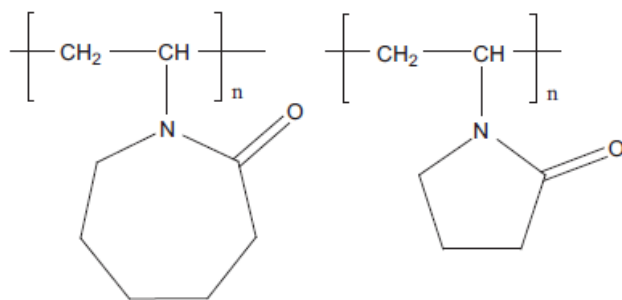


Figure 19 Structure of VC/VP copolymer [36]

3.2.4 Procedure

The kettle was filled with 1 L 0.1 wt% NaCl in distilled water. In some of the experiments 5000 ppm Luvicap 55W was added without any oil phase present. The solution was heated to 70 °C and purged with CO₂ gas for one hour to achieve full saturation and proper stabilization of the system. Electrodes were inserted after one hour and the LPR measurements started. The metal coupons were allowed to corrode for one hour before Cl was added. Stirring rate and gas flow was adjusted prior the addition of the Cl to decrease turbulence which potentially may lead to low film forming rate. The test ran for 23 hours from start to end. Test conditions are summarized in table 4.

Table 4 Test conditions in corrosion testing

	Stabilizing period	Before adding Cl
Temperature (°C)	70	70
Stirring (rpm)	300	150
Flowrate (ml/min)	400	250

To avoid variations and get more reproducible results the same kettle, hotplate and probe/channel was used for each parallel.

PC set up was done according to M-I SWACO test standard with parameters set at standard conditions.

Corrosion rate was calculated and recorded by the software Sequencer/ Version 5 and V4 Analysis Software/version 5 (Copyright ACM Instruments 2001).

3.3 Hydrate testing

To investigate CIs effects on Luvicap 55W, hydrate tests were performed in a RCS rig from PSL. The software “PSL Technik Win RCS “was included in the rig computer. Test procedure was performed accordingly to M-I SWACO’s test standard. Test standard was not included in appendix due to proprietary information.

3.3.1 Equipment

The hydrate RCS record pressure, temperature and runtime data from 6 cells which are pressurized and put to rock in the bath. The cells consist of a metal housing and a clear sapphire tube (figure 20). Inside the sapphire tube a steel ball is moving back and forth as the cells are rocked with a set angle.

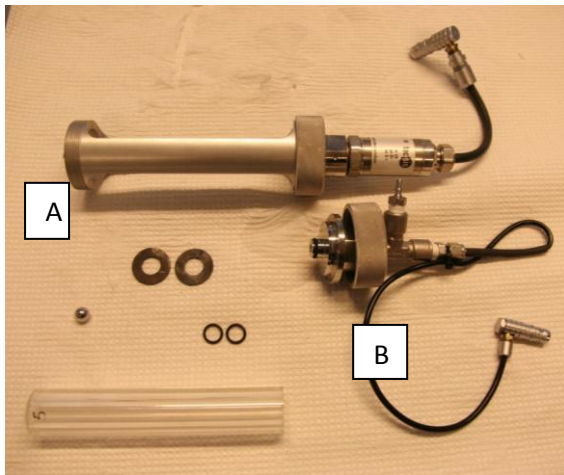


Figure 20 Parts in a hydrate test cell

The housing (A) is where the glass tube is inserted. At the end of it a pressure transmitter is present. The top lid (B) includes the pressure line connector and a temperature sensor at the end. The mixing ball, sapphire glass tube and o-rings are also in the picture.

Figure 21 show the configuration of two cells that are connected in the rig. The orange tubing is the pressure line.



Figure 21 Cells connected in the RCS

The bath temperature is set to the desirable temperature and is cooled down by an external cooling unit. Adjustments in the software allow various settings so different pipeline situations can be simulated.

3.3.1.1 Chemicals

It was decided to leave out the concentration below the CMC for each CI in order to save experiments. The test concentrations for each chemical are summarized in table 5.

Table 5 Test concentrations in hydrate testing

Corrosion Inhibitor	At CMC	Above CMC	Luvicap 55W	NaCl
Imidazoline A	30 ppm	80 ppm	5000 ppm	0.1 wt%
Imidazoline B	25 ppm	50 ppm	5000 ppm	0.1 wt%
Fatty Acid derivate	20 ppm	70 ppm	5000 ppm	0.1 wt%

Two replicates for each CI concentration was carried out. The baseline for Luvicap 55W was tested alone with three replicates. Induction time was compared in all of the tests.

3.3.1.2 Gas mixture

Gas composition for the mixed gas employed in the experiments is presented in table 6. This gas mix results in sll hydrates due to the composition including propane and butane.

Table 6 Gas composition

Gas type	Gas mix (G11)
Methane	85,29
Ethane	4,18
Propane	5,37
Isobutane	1,49
n- Butane	2,60
Nitrogen	0,13
Carbondioxide	0,94

For the specific gas, the phase envelope (figure 22) was simulated with Multiflash for Windows (32 bit), Version 3.8. Copyright (C) 2008 (Infochem Computer Services Ltd). Pressure is represented at the Y-axis and temperature is at the X-axis. A bigger format of this P-T graph is found in appendix 2.

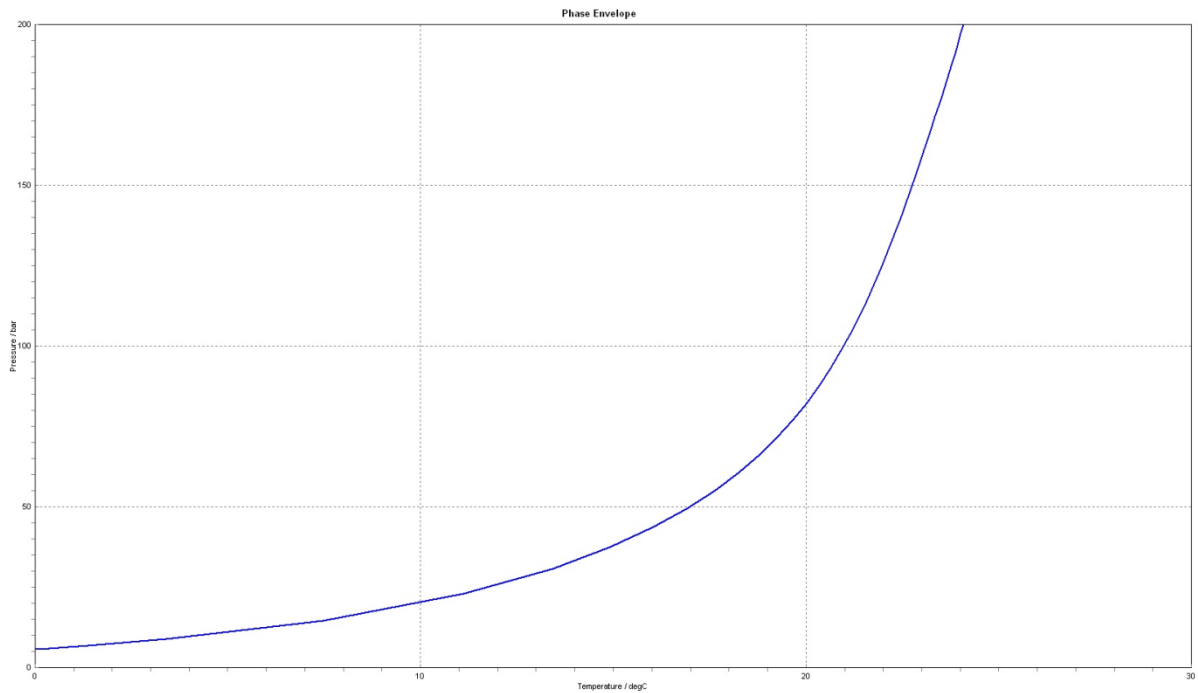


Figure 22 P-T diagram simulating the phase envelope of gas mixture G11 with 0.1% NaCl

Set temperature for the experiment was 4.3 °C and test pressure was 32±0.5 bars which result in a sub-cooling at 9±0.5 °C.

3.3.1.3 Test conditions

Test conditions for the hydrate experiments are presented in table 7.

Table 7 Test conditions in hydrate testing

Start temperature	12 °C
End temperature	4.3 °C
Sub-cooling	9 °C
Pressure	32 bar
Run time at 4 C	24 h
Rocking rate (sec)	5''-0''-5''
Cycles/min	12
Rocking angle	40 °

3.3.2 Procedure

10 ml sample was filled in the cells. The cells were connected properly in the hydrate RCS rig. The cells were flushed three times with gas prior the pressurization. As the experiment was terminated the cells were depressurized and disconnected. Properly and thorough cleaning was needed to remove as much CI as possible prior a new experiment. The sapphire tubes were washed with soap, lots of warm water, distilled water and then lots of acetone. The sensors in the housings were also washed thorough. As corrosion inhibitors was added in the tests even more acetone was needed compared to when only KHIs is present. The sapphire tubes were immersed in acetone for 2 hours after washing. The o-ring in the housing and the lid had to be changed after each experiment.

The sapphire tubes, housing and lid were numbered to reduce the relocation possibilities and continuance of existing error in the same cell number.

4 RESULTS AND DISCUSSION

4.1 Surface tension

Surface tension was measured with a Kruss tensiometer by the DuNoüy-ring method. 40 ml of 0.1 wt% NaCl and 5000 ppm (0.5 %) Luvicap 55W solution with various concentrations of CI was mixed and held static for 24 hours before the measurements took place. Corrosion inhibitor concentrations and surface tension measurements are summarized in table 8.

Table 8 Corrosion inhibitor concentration and surface tension values (± 1.0 mN/m)

Imidazoline A		Imidazoline B		Fatty Acid derivate	
ppm	mN/m	ppm	mN/m	ppm	mN/m
5	42	5	44	5	37
10	38	10	39	8	36
20	36	20	36	10	31
30	33	30	34	15	31
50	33	50	34	30	28
100	31	100	33	50	28
300	31	300	33	100	28
500	31	500	33	300	28
				500	28

Measured surface tension (± 1.0 mN/m) was reported versus CI concentration. CMC were found in the intersection of the two lines that were formed. The graphs are presented in figure 23-25.

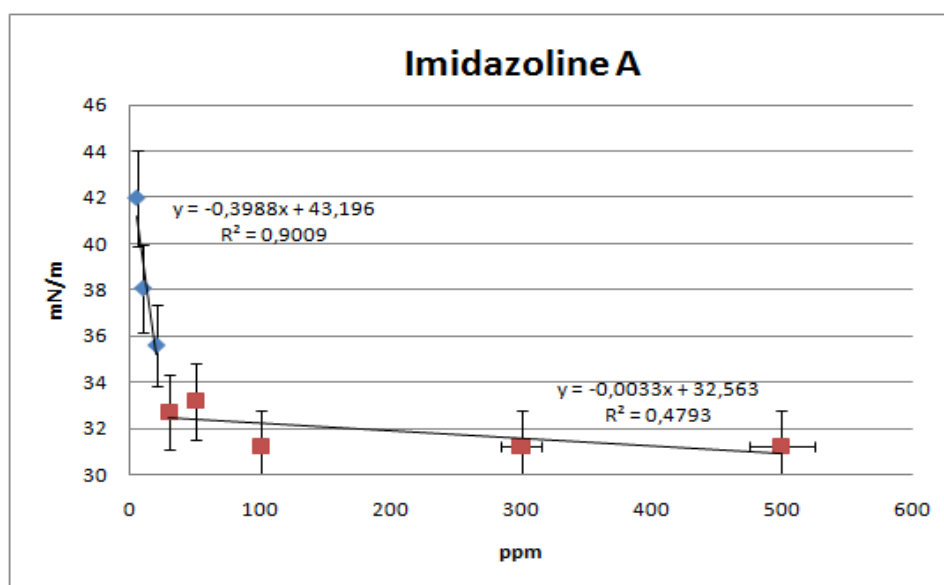


Figure 23 Surface tension for Imidazoline A at different concentrations and 0.5 % Luvicap 55W

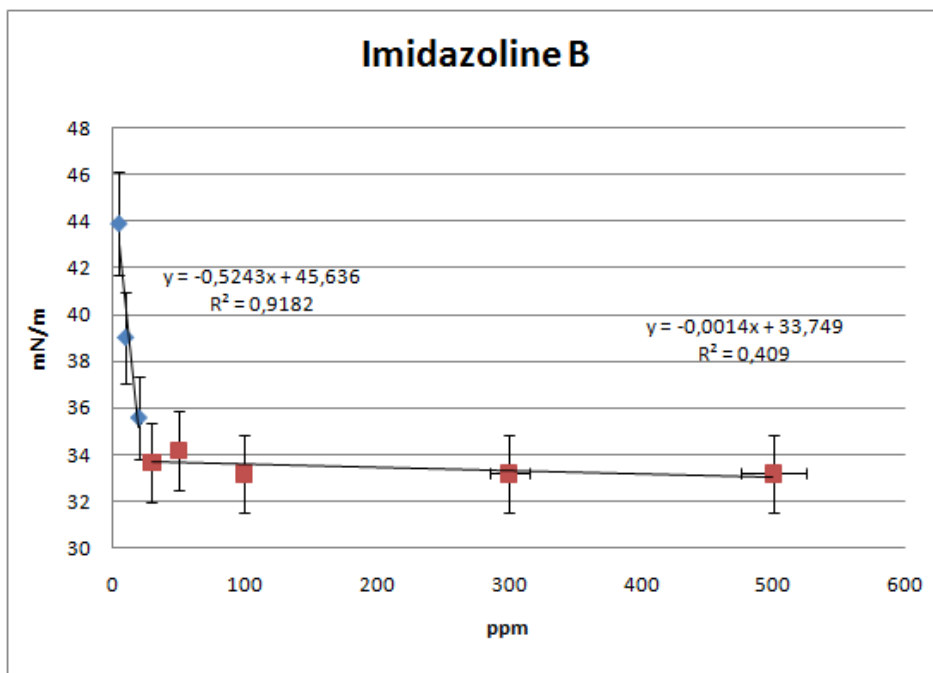


Figure 24 Surface tension for Imidazoline B at different concentrations and 0.5% Luvicap 55W

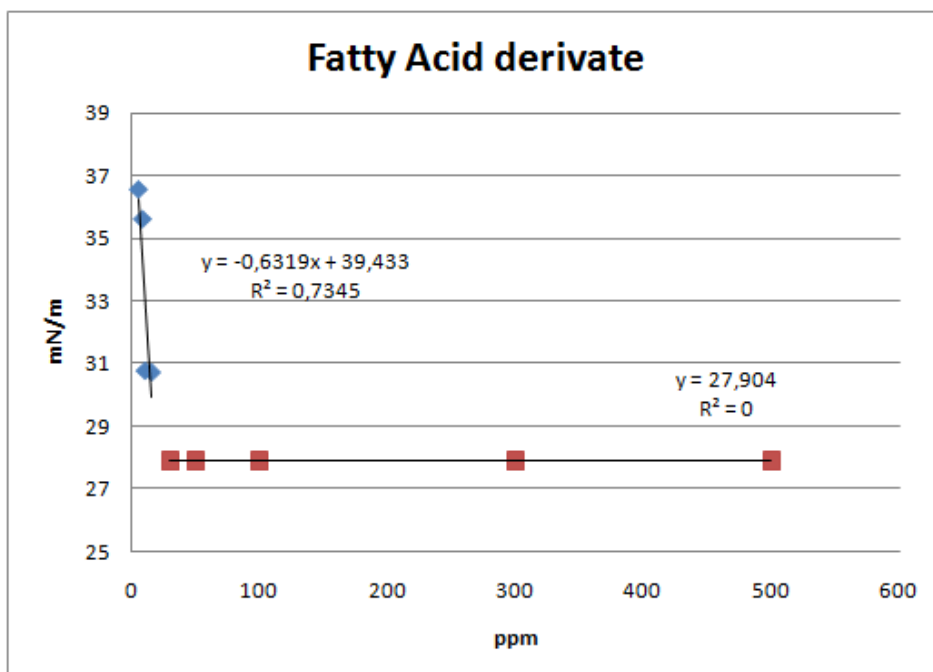


Figure 25 Surface tension for Fatty Acid der. at different concentrations and 0.5% Luvicap 55W

CMC for each solution was approximated in fives and summarized in table 9.

It was of interest to check interaction between the corrosion inhibitor and the hydrate inhibitor at three different concentrations; below the CMC, at the CMC and above the CMC which were chosen randomly.

Table 9 CMC for each CI and selected test concentrations

	Imidazoline A	Imidazoline B	Fatty Acid derivate
Below CMC	10 ppm	10 ppm	5 ppm
CMC	30 ppm	25 ppm	20 ppm
Above CMC	80 ppm	50 ppm	70 ppm

4.1.1 Discussion

The curves created from measuring surface tension in fatty acid solution were more consistent than for the Imidazoline's. This resulted in a more precise CMC value.

After evaluating corrosion test results it was discovered that CMC for each solution probably was affected by the polymer (Luvicap 55W). The CIs performance was expected to be higher in the corrosion tests without KHI present.

Normal dosage of a corrosion inhibitor in the field is approximately 20-30 ppm, which are normally obtained from CMC measurements [13].

When polymers are present with a surfactant, they tend to impact the CMC for the solution due to a polymer-surfactant interaction [37].

4.2 Corrosion Testing

Corrosion testing was performed by using LPR technique. At least three replicates were performed. In some of the tests it was discovered traces of Cl which resulted in decreasing corrosion rate prior the addition of Cl. These data were rejected and a new test was carried out. The solute was made of 0.1 wt% NaCl. Interactions was revealed by comparing Cl efficiency in presence of Luvicap 55W and without it.

Corrosion rate was calculated and recorded by the software Sequencer/ Version 5 and V4 Analysis Software/version 5 (Copyright ACM Instruments 2001).

Cl efficiency was calculated at 15 hour in all of the tests by using equation 4.

$$\% \text{ inhibition efficiency: } \left(\frac{R_0 - R_1}{R_0} \right) \times 100\% \quad (4)$$

Where:

R_0 = corrosion rate without inhibitor

R_1 = corrosion rate with inhibitor at 15 hours.

4.2.1 Imidazoline A

A lot of foam was created in the tests especially when Luvicap 55W was present. This resulted in some liquid loss and probably inhibitor loss.

4.2.1.1 10 ppm

Performance of 10 ppm Imidazoline A in presence of 0.5 % Luvicap 55W and without is presented in figure 26 and 27.

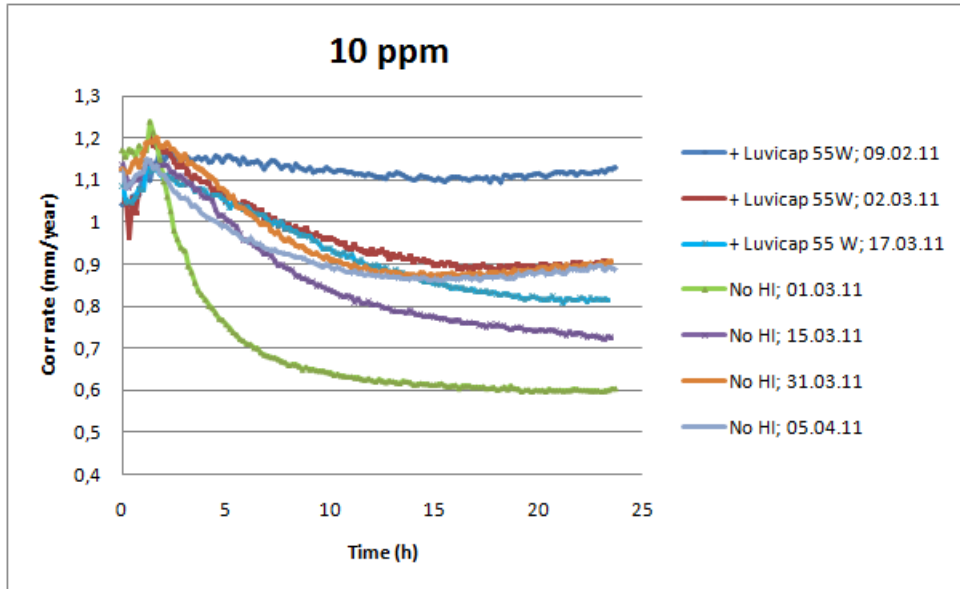


Figure 26 Performance of 10 ppm Imidazoline A

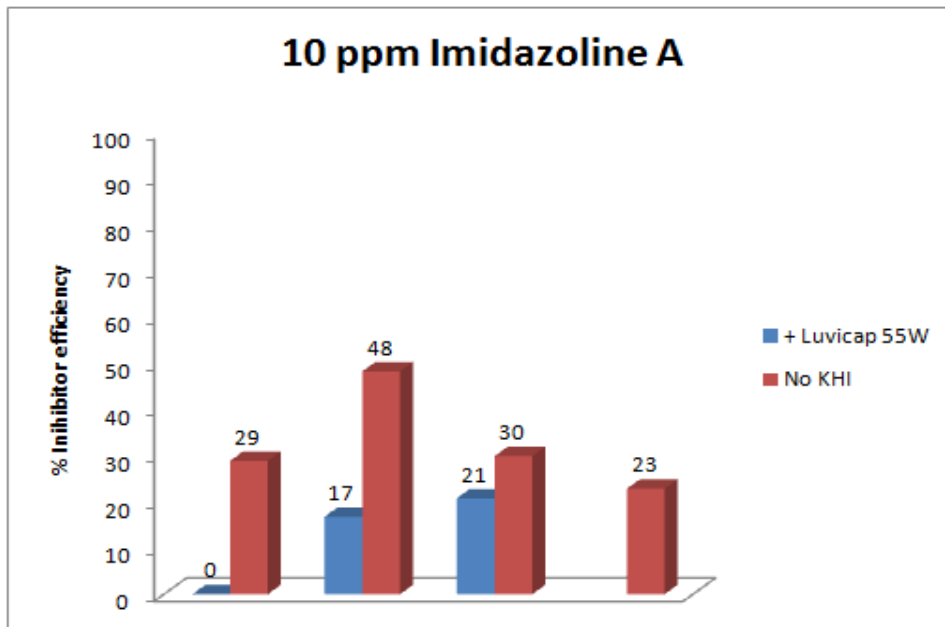


Figure 27 Percent efficiency of Imidazoline A

4.2.1.2 30 ppm

Performance of 30 ppm Imidazoline A in presence of 0.5 % Luvicap 55W and without is presented in figure 28 and 29.

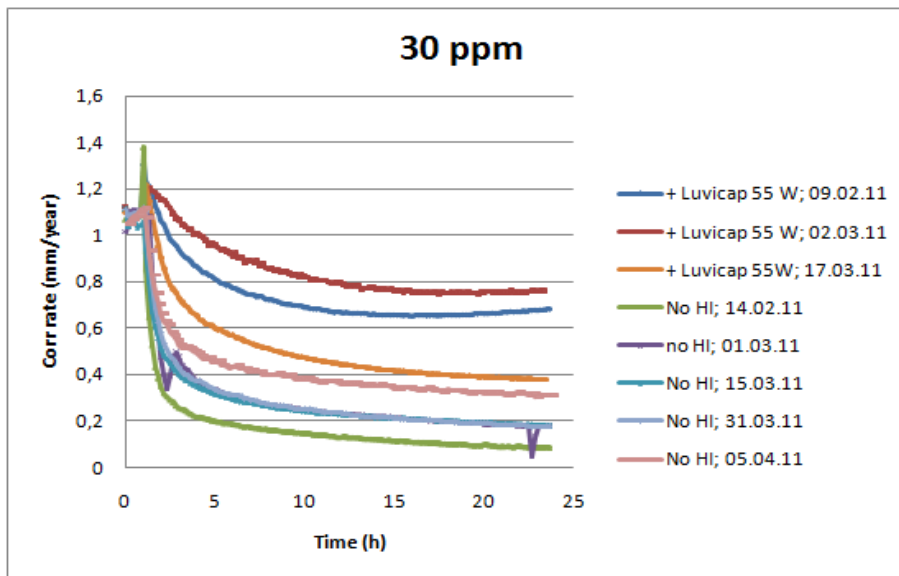


Figure 28 Performance of 30 ppm of Imidazoline A

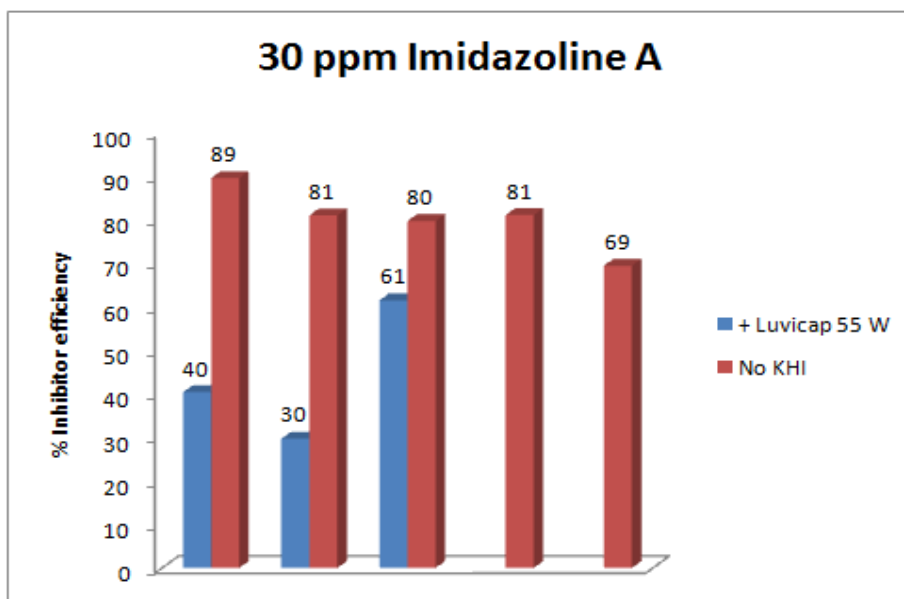


Figure 29 Percent efficiency of Imidazoline A with and without the presence of Luvicap 55W

4.2.1.3 80 ppm

Performance of 80 ppm Imidazoline A in presence of 0.5 % Luvicap 55W and without is presented in figure 30 and 31.

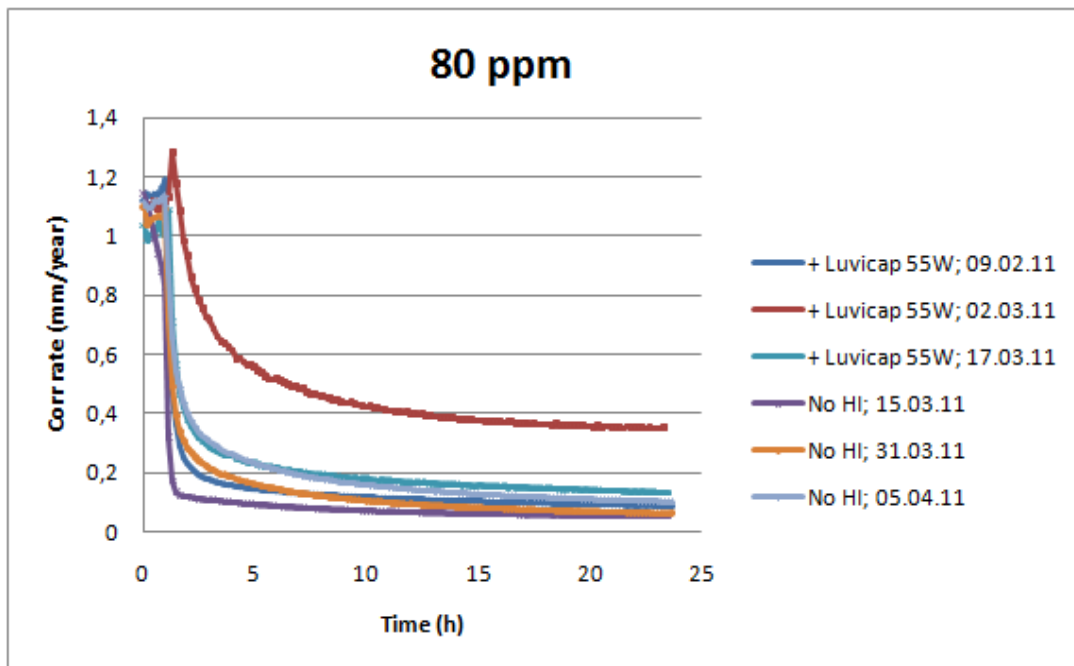


Figure 30 Performance of 80 ppm of Imidazoline A

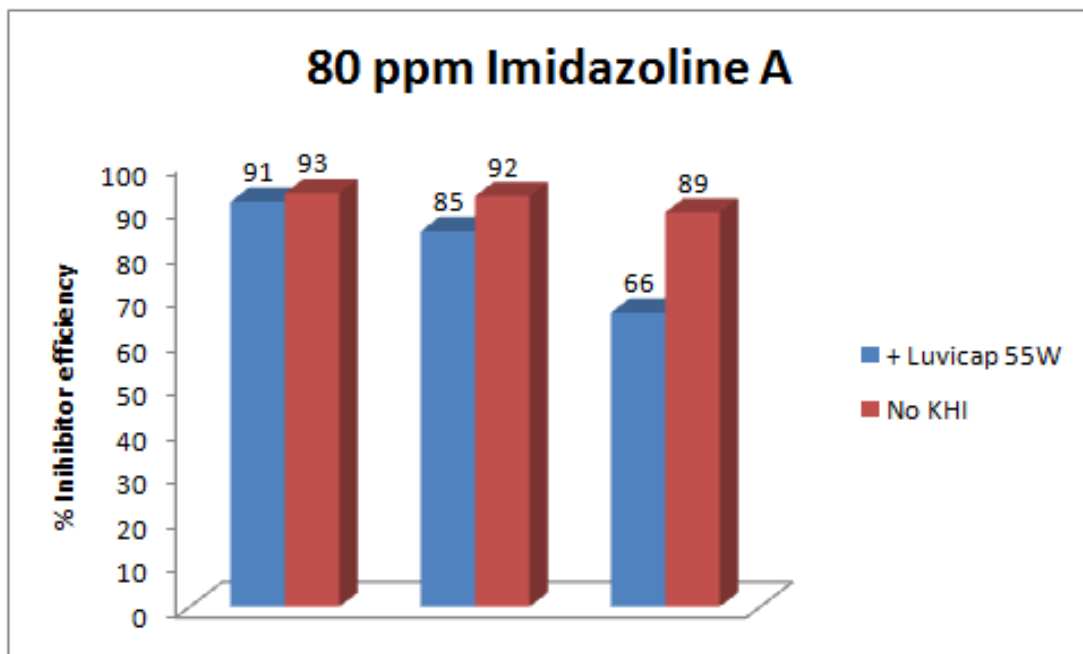


Figure 31 Percent efficiency of Imidazoline A at 80 ppm

Average and standard deviation (SD) for the replicates at 15 h was calculated and are summarized in table 10. The standard deviation indicated that the reproducibility was poor in the tests. SD was particularly large in tests with Luvicap 55W present.

Table 10 Average performance and standard deviation for the replicates

ppm	No KHI (Average)	SD	+ KHI (Average)	SD
10	34	13,11	13	11,04
30	83	7,16	44	16,16
80	91	2,33	81	12,94

Figure 32 show the average inhibitor efficiency presented graphically.

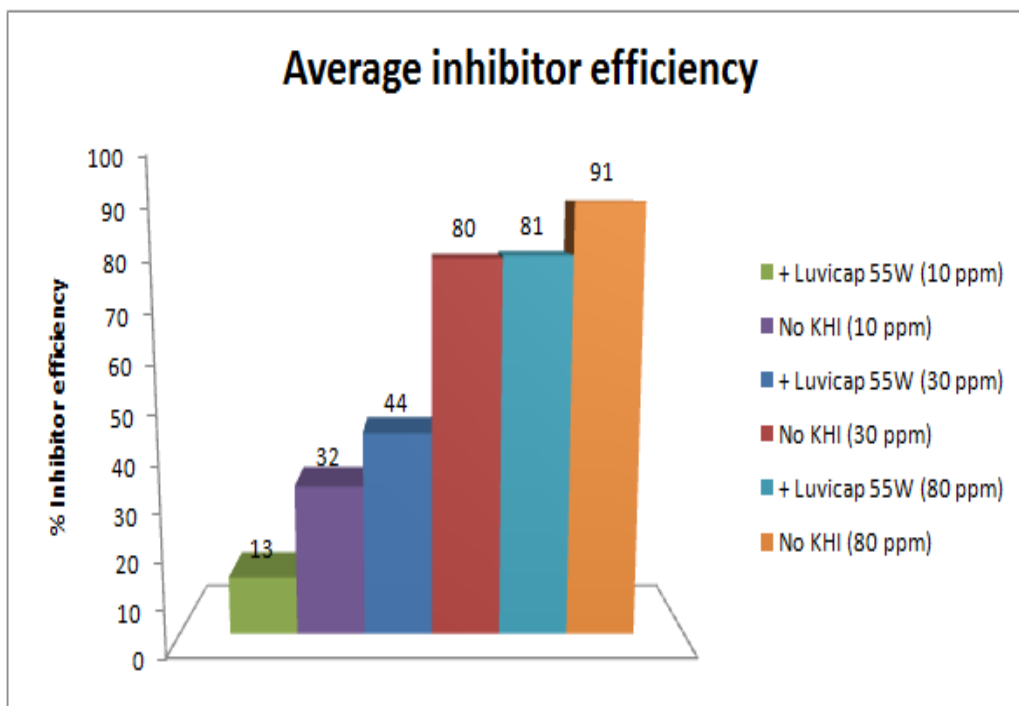


Figure 32 Average of the inhibitor efficiency

Despite poor reproducibility, a trend of decreased CI performance in presence of Luvicap 55W was seen: 55 % reduction for CI at CMC and 11 % reduction when CI was added above CMC.

4.2.2 Imidazoline B

Lots of foam was produced in the tests especially when Luvicap 55W was present. Reproducibility was poor but a little higher than in the tests with Imidazoline A.

4.2.2.1 10 ppm

Performance of 10 ppm Imidazoline B in presence of 0.5 % Luvicap 55W and without is presented in figure 33 and 34.

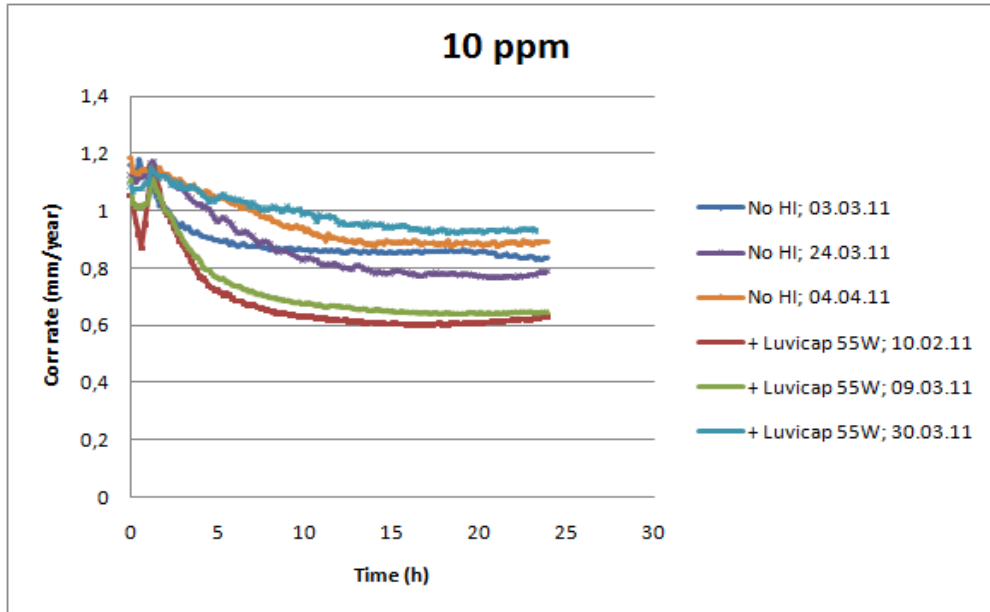


Figure 33 Performance of 10 ppm Imidazoline B

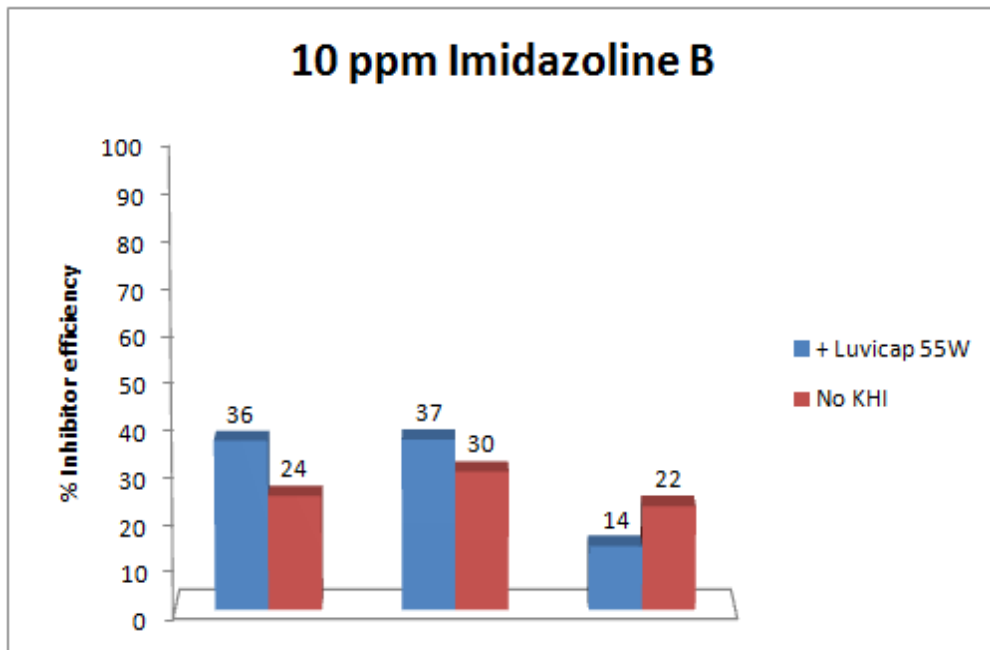


Figure 34 Percent inhibitor efficiency of 10 ppm Imidazoline B

4.2.2.2 25 ppm

Performance of 25 ppm Imidazoline B in presence of 0.5 % Luvicap 55W and without is presented in figure 35 and 36.

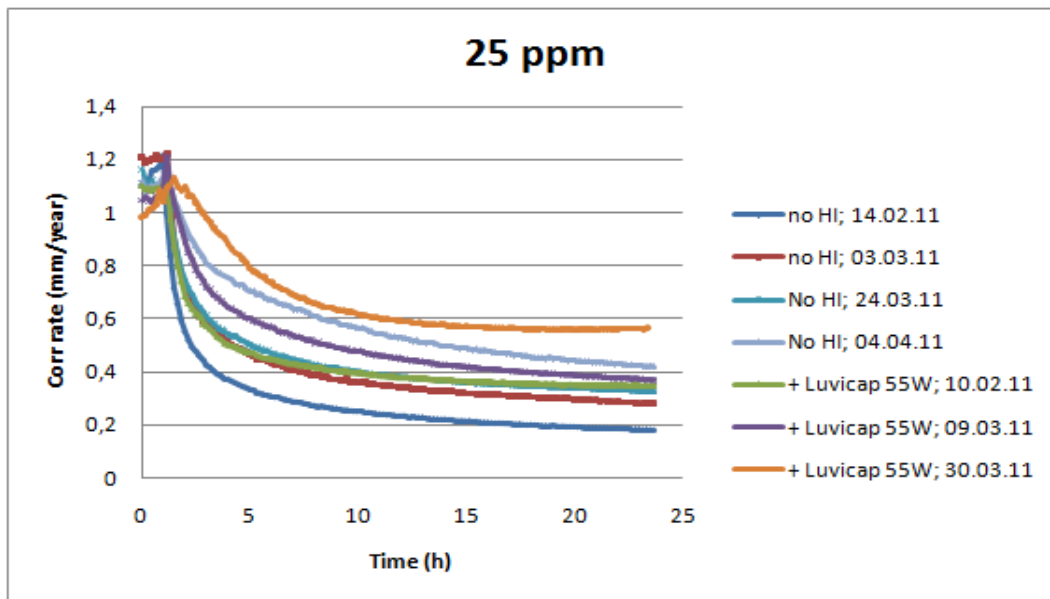


Figure 35 Performance of 25 ppm Imidazoline B

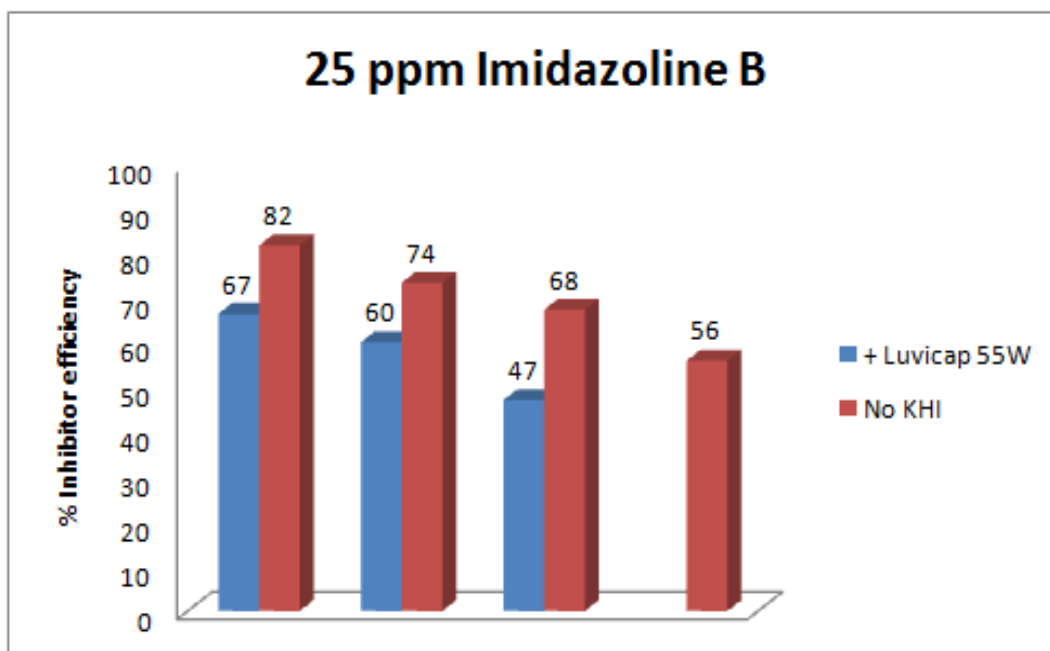


Figure 36 Percent inhibitor efficiency of 25 ppm Imidazoline B

4.2.2.3 50 ppm

Performance of 25 ppm Imidazoline B in presence of 0.5 % Luvicap 55W and without is presented in figure 37 and 38.

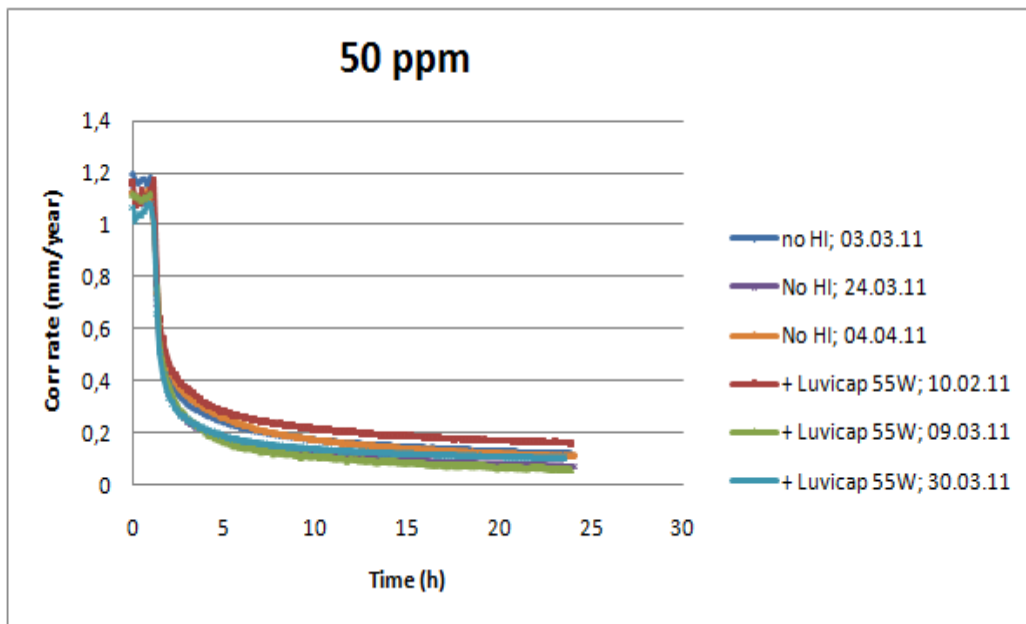


Figure 37 Performance of 50 ppm Imidazoline B

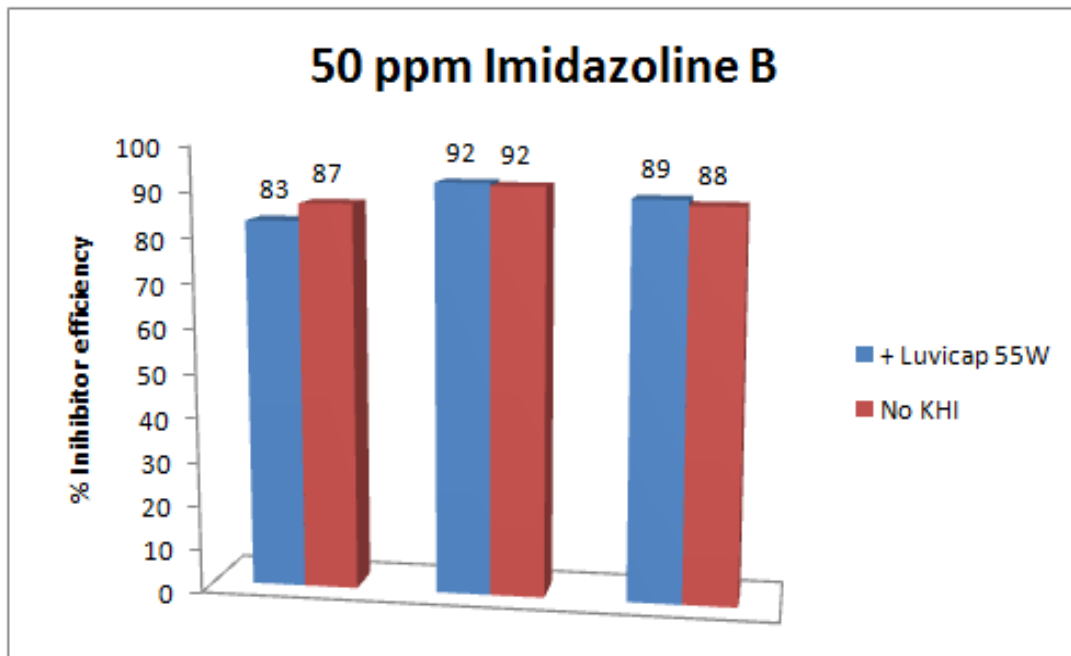


Figure 38 Percent inhibitor efficiency of 50 ppm Imidazoline B

Average and SD for the average inhibitor performance was calculated (table 11). Large SD's emphasized the poor reproducibility in the tests.

Table 11 Average performance and standard deviation for Imidazoline B replicates

ppm	No KHI (Average)	SD	+KHI (Average)	SD
10	26	3,85	29	13,17
25	70	10,86	58	9,85
50	89	2,34	88	4,51

Figure 39 show the average inhibitor efficiency presented graphically.

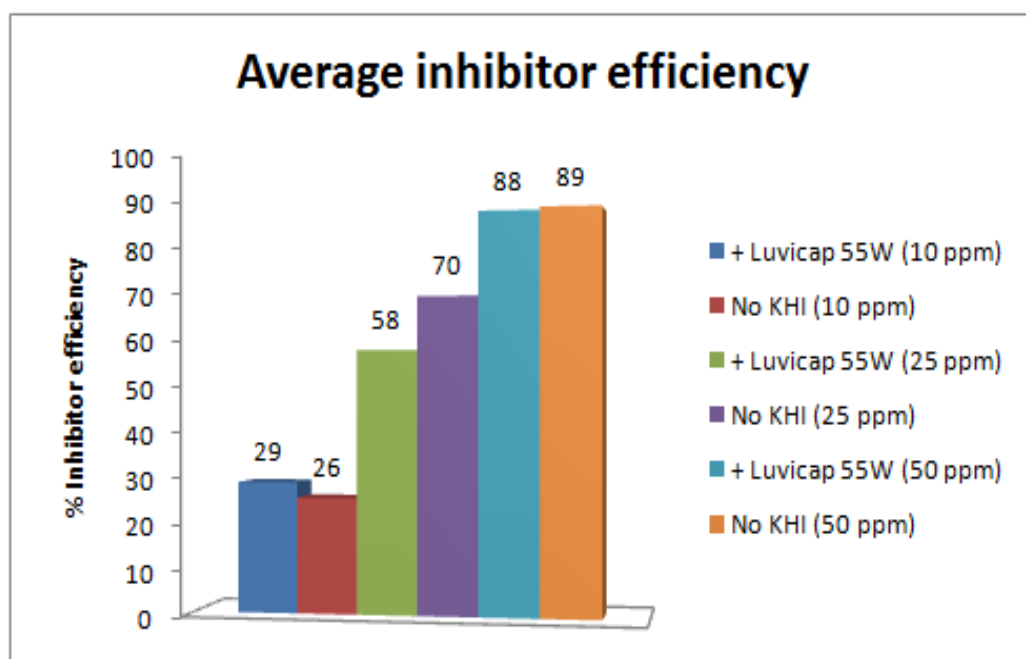


Figure 39 Average efficiency of Imidazoline B

Imidazoline B performance was decreased with 12 % (at CMC) and 1 % (above CMC).

4.2.3 Fatty Acid derivate

No foam was produced in the tests. Reproducibility was higher for this CI especially at higher concentrations.

4.2.3.1 5 ppm

Performance of 5 ppm fatty acid derivate in presence of 0.5 % Luvicap 55W and without is presented in figure 40 and 41. Reproducibility among the replicates was poor.

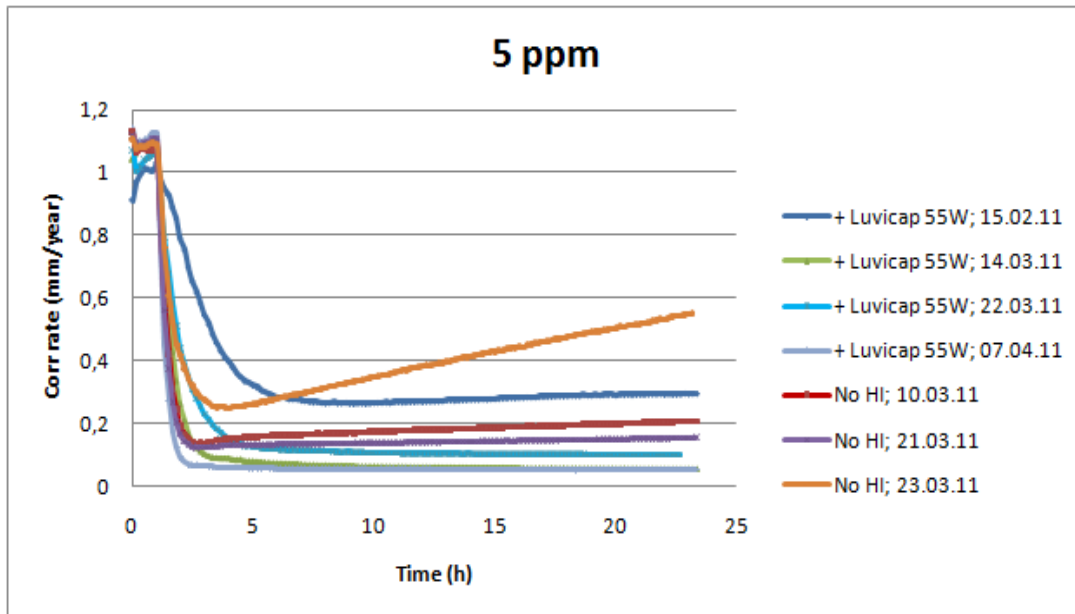


Figure 40 Performance of 5 ppm fatty acid derivate

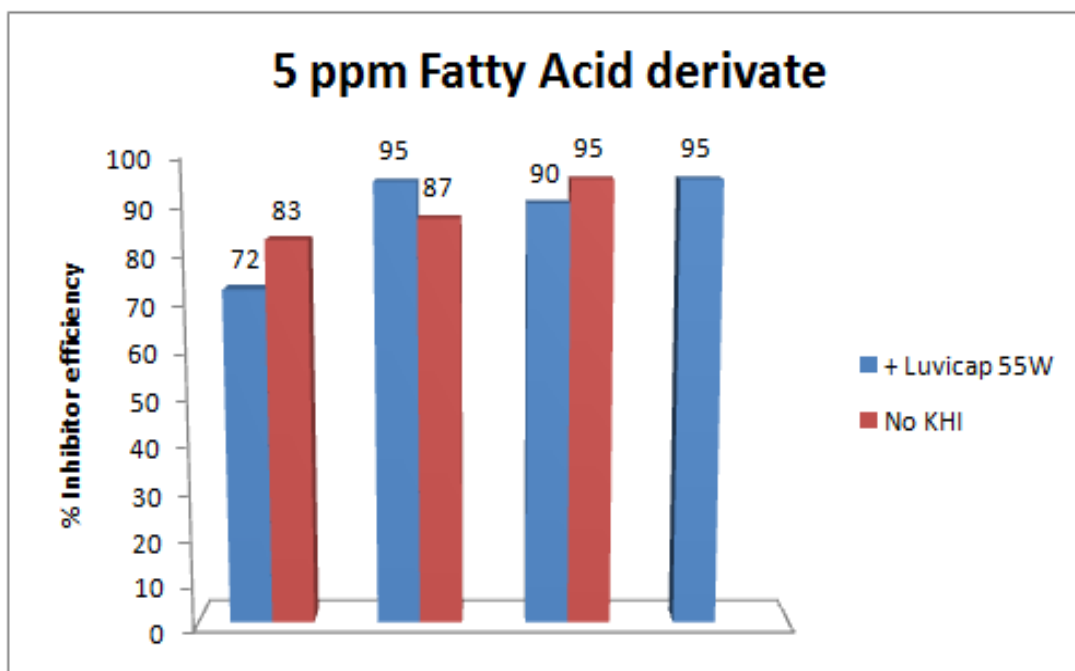


Figure 41 Percent inhibitor efficiency of 5 ppm fatty acid derivate

4.2.3.2 20 ppm

Performance of 20 ppm fatty acid derivate in presence of 0.5 % Luvicap 55W and without is presented in figure 42 and 43.

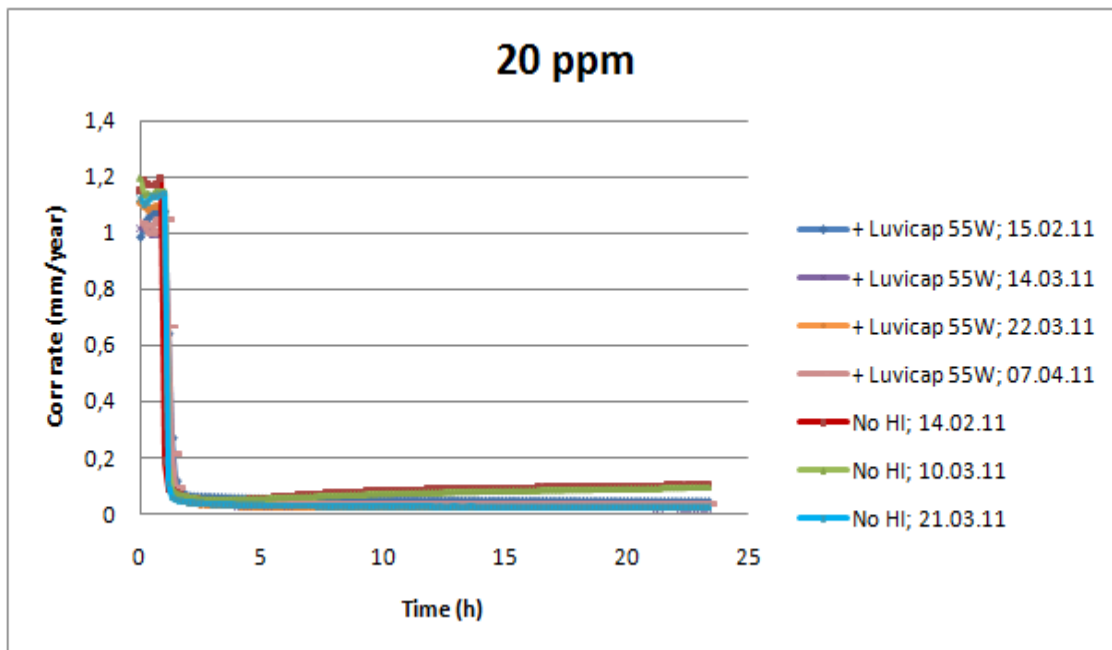


Figure 42 Performance of 20 ppm fatty acid derivate

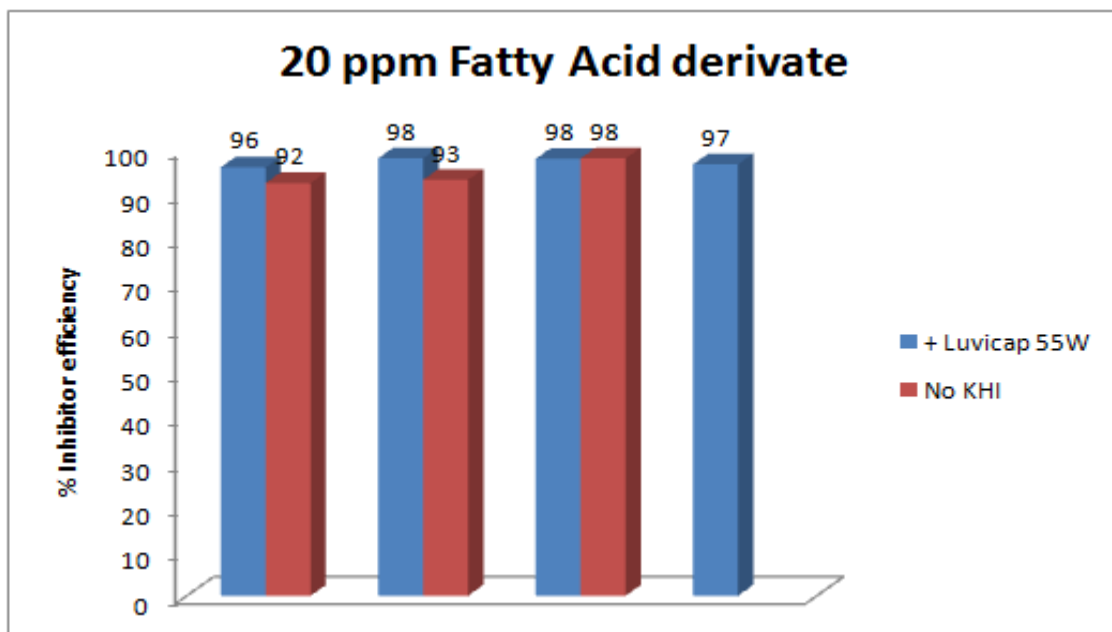


Figure 43 Percent inhibitor efficiency of 20 ppm fatty acid derivate

4.2.3.3 70 ppm

Performance of 25 ppm Imidazoline B in presence of 0.5 % Luvicap 55W and without is presented in figure 44 and 45.

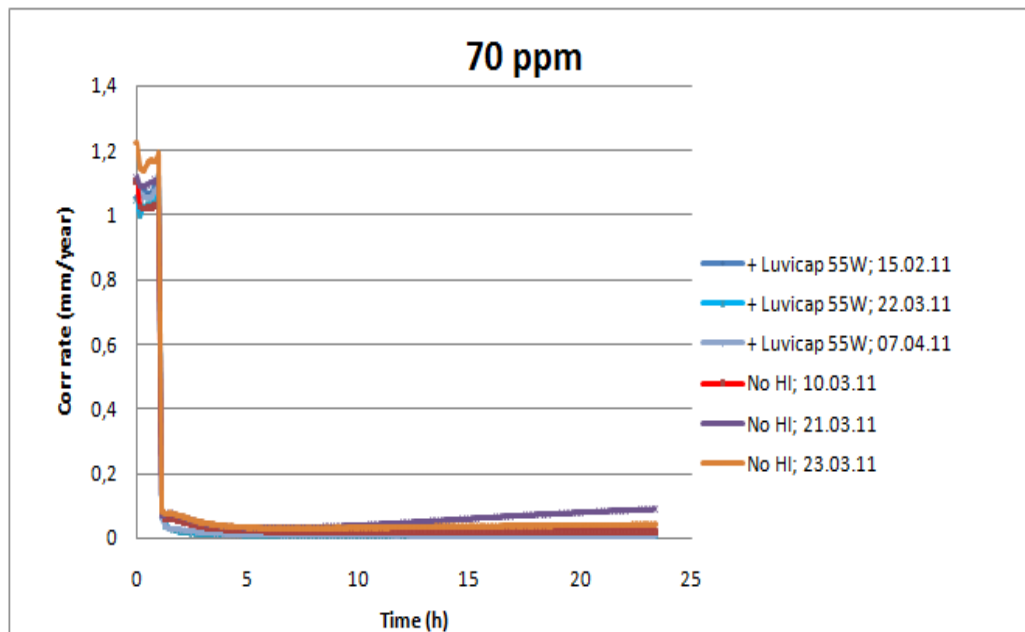


Figure 44 Performance of 5 ppm fatty acid derivate

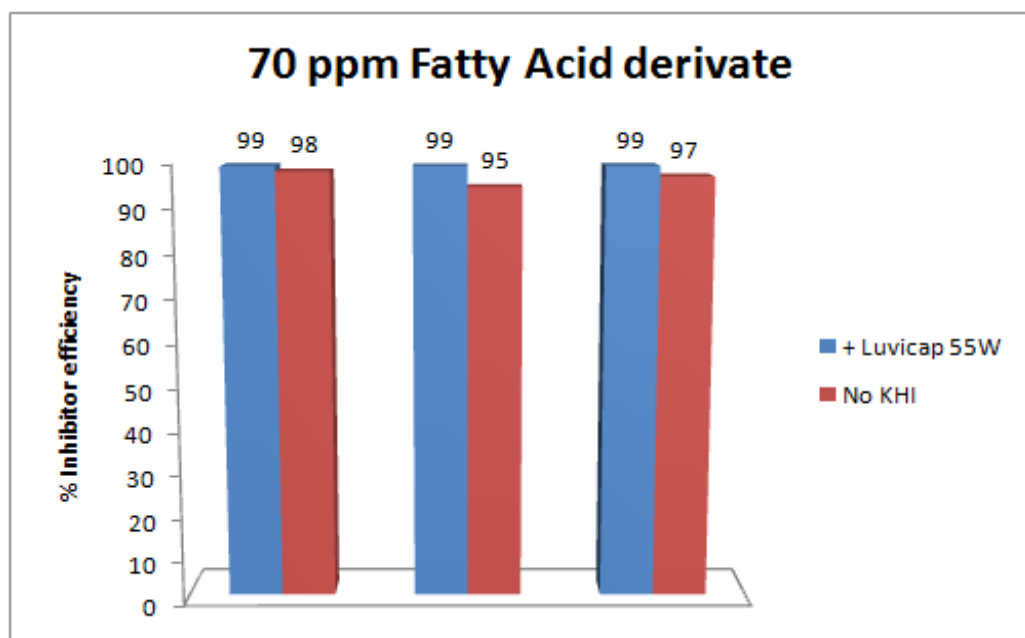


Figure 45 Percent inhibitor efficiency of 70 ppm fatty acid derivate

Average for the inhibitor performance and SD was calculated (table 12).

Table 12 Average and standard deviation for fatty acid derivate

ppm	No HI (average)	SD	HI (average)	SD
5	88	6,44	88	10,88
20	94	3	97	0,98
70	97	1,79	99	0,03

The average from table 5 was presented graphically in figure 46. Results from table 12 indicated that Luvicap 55W increased CI performance with respectively 3 % (at CMC) and 2 % (above CMC).

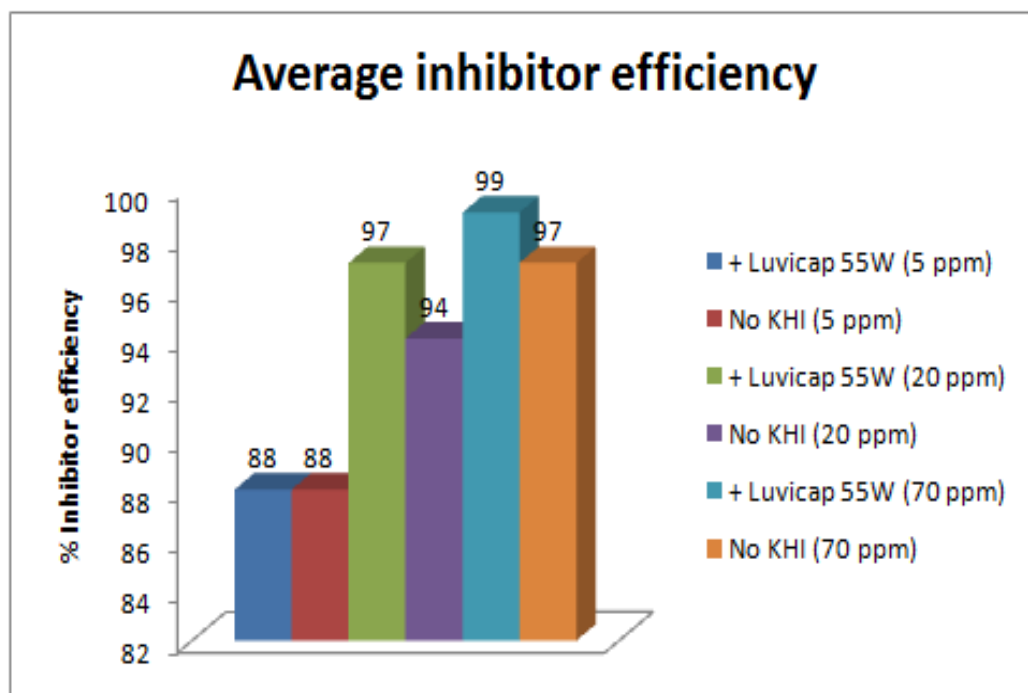


Figure 46 Average performance of fatty acid derivate

Based on the average inhibitor efficiency (table 10, 11 and 12), the rate of change (Δ) in performance was found. Table 13 summarizes the Δ performance for all three CI's. Minus sign emphasize the decreasing performance of CI when Luvicap 55W was present whereas positive Δ represent increased performance.

Table 13 Performance change of CIs in presence of Luvicap 55W

Imidazoline A	Δ Performance
10	-21
30	-39
80	-10
Imidazoline B	
10	3
25	-12
50	-1
Fatty acid derivate	
5	0
20	3
70	2

4.2.3.4 Summary

Foam was produced in the corrosion tests with Imidazoline A and B. The foaming problems increased with Luvicap 55W present. This resulted in some liquid loss and maybe in chemical loss. Fatty acid derivate didn't foam.

Results indicated that the performance of Imidazoline A was more reduced in presence of Luvicap 55W than Imidazoline B.

Fatty acid derivate performance was slightly improved when Luvicap 55W was present.

Test results in the mixtures above CMC were more consistent than at CMC and below. This clearly emphasizes the importance of finding CMC for a surfactant solution. Over dosage is usually done in a system to ensure protection against corrosion.

4.3 Hydrate testing

The hydrate testing was performed in a hydrate RCS. Some of the pressure sensors were not working properly in the rig, which resulted in two replicates for each test mixture.

CMC and the concentration above CMC were tested in solution with 0.5 % Luvicap 55W and 0.1 wt% NaCl. Hydrate induction time was compared with the baseline (0.5 % Luvicap 55W in 0.1 % NaCl) to reveal possible interactions between the KHI and CIs.

Since hydrate formation is a stochastic process the first observed induction time was decided to define the chemical performance level because of the low number of replicates.

Hydrates were formed in all of the tests. Figure 47 is a picture taken from one of the cells blocked with a gas hydrate.



Figure 47 Formed gas hydrate in one of the tests

4.3.1 Luvicap 55W

The baseline for 0.5 wt% Luvicap 55W without any CI was tested in a triplicate (figure 48). Hydrates were formed in all three tests.

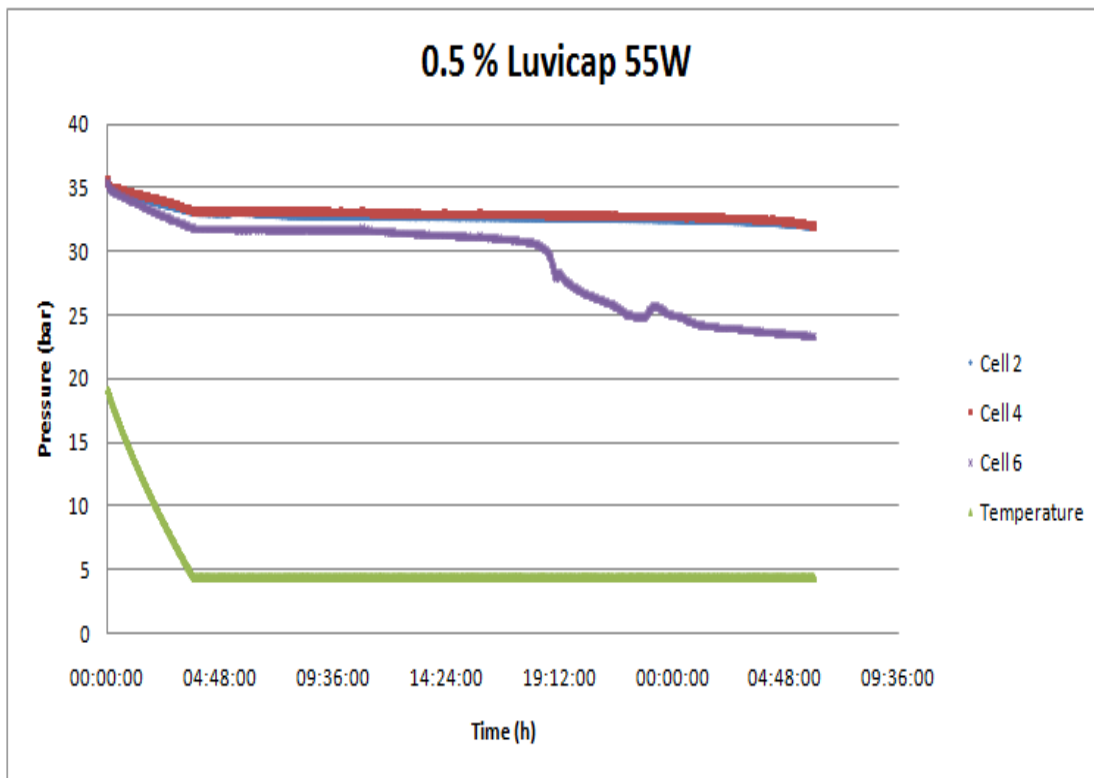


Figure 48 Performance of 0.5 % Luvicap 55W tested in a hydrate RCS

4.3.2 Imidazoline A

Figure 49 and 50 show the results of the gas hydrate test with Imidazoline A in presence of 0.5 % Luvicap 55W.

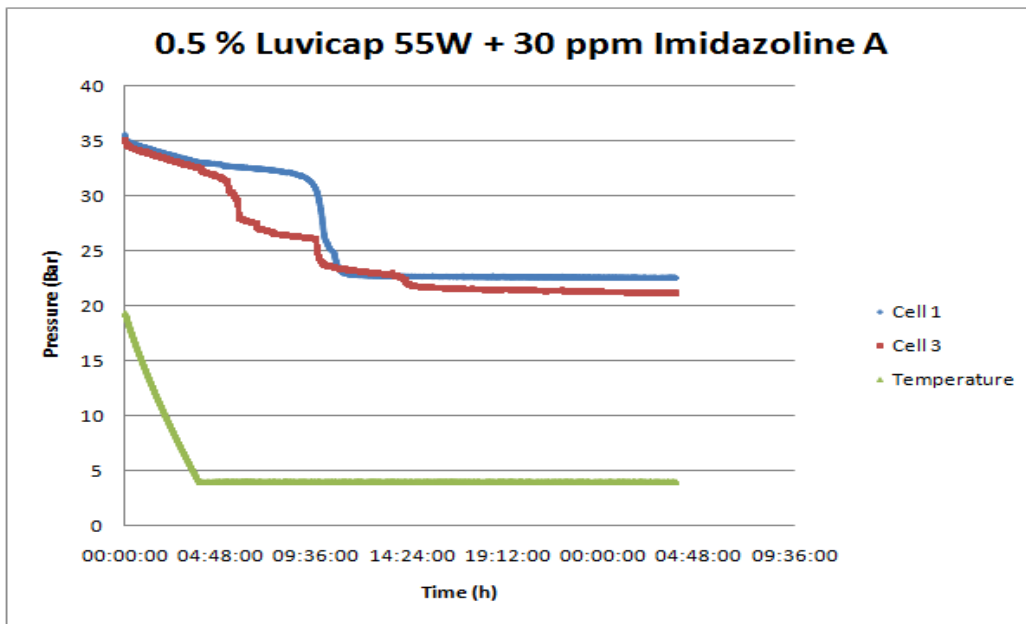


Figure 49 Performance of Luvicap 55W in presence of 30 ppm Imidazoline A

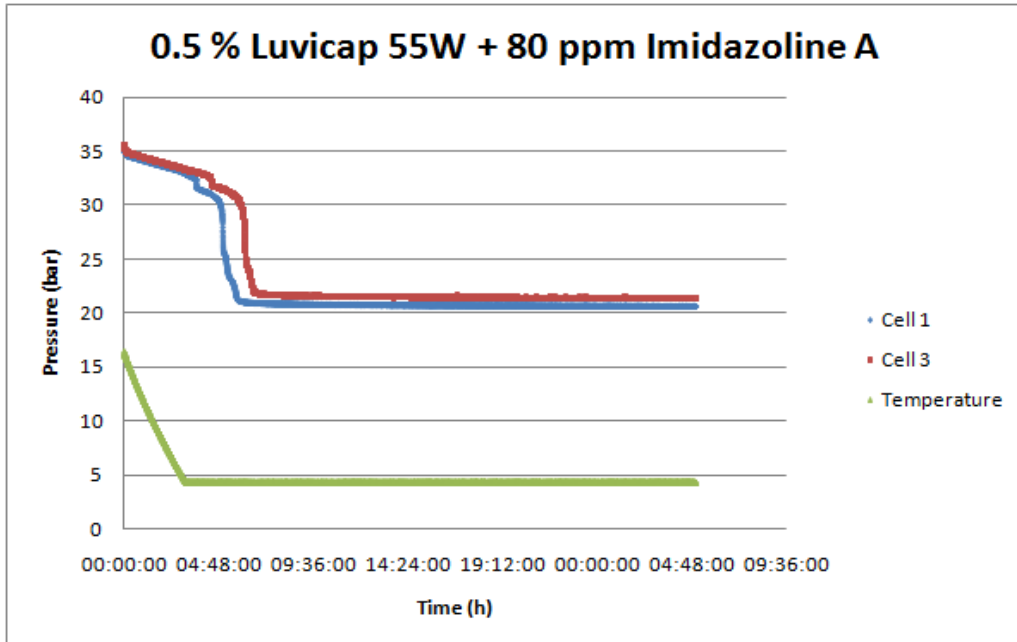


Figure 50 Performance of Luvicap 55W in presence of 80 ppm Imidazoline A

4.3.3 Imidazoline B

Figure 51 and 52 show the results of the gas hydrate test with Imidazoline B in presence of 0.5 % Luvicap 55W.

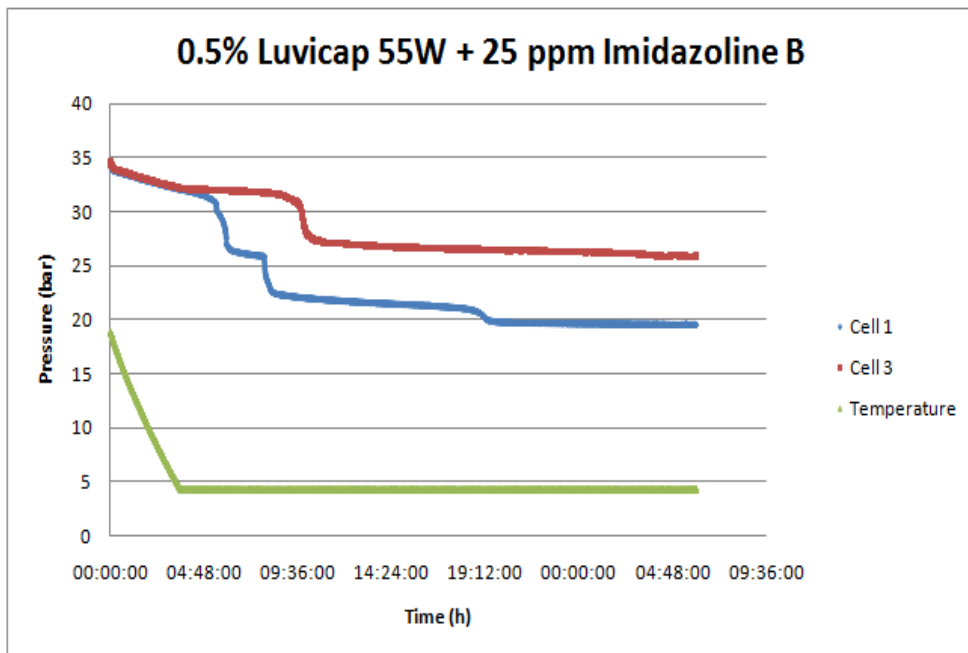


Figure 51 Performance of Luvicap 55W in presence of 25 ppm Imidazoline B

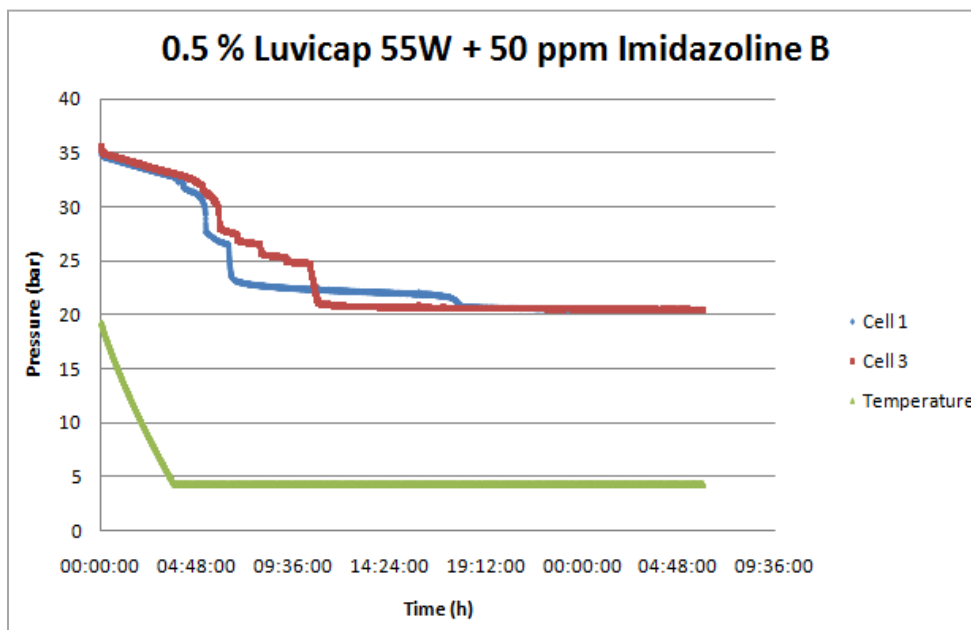


Figure 52 Performance of Luvicap 55W in presence of 50 ppm Imidazoline

4.3.4 Fatty Acid derivate

Figure 53 and 54 show the results of the gas hydrate test with fatty acid derivate in presence of 0.5 % Luvicap 55W.

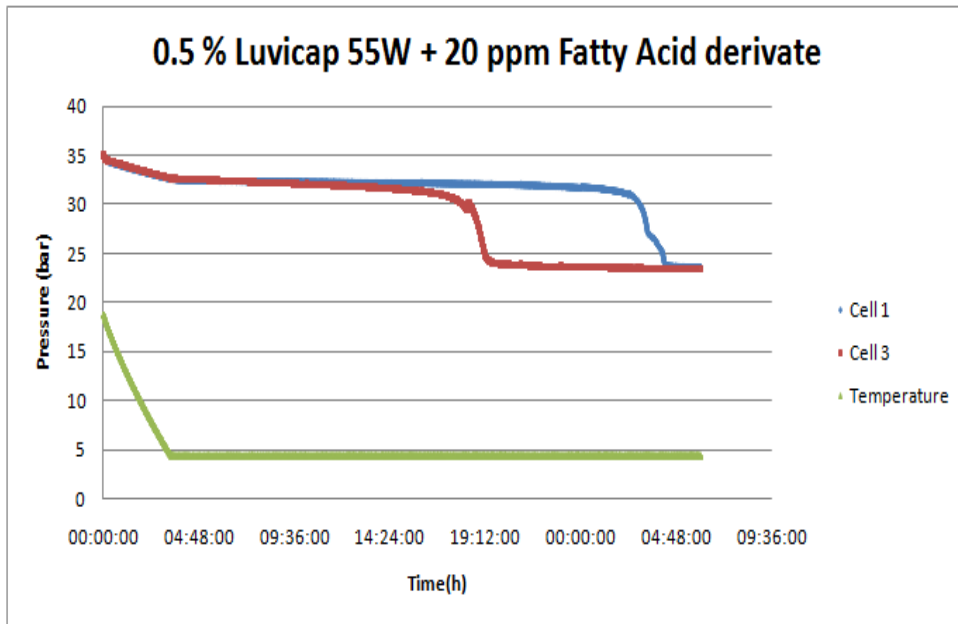


Figure 53 Performance of Luvicap 55W in presence of 20 ppm fatty acid derivate

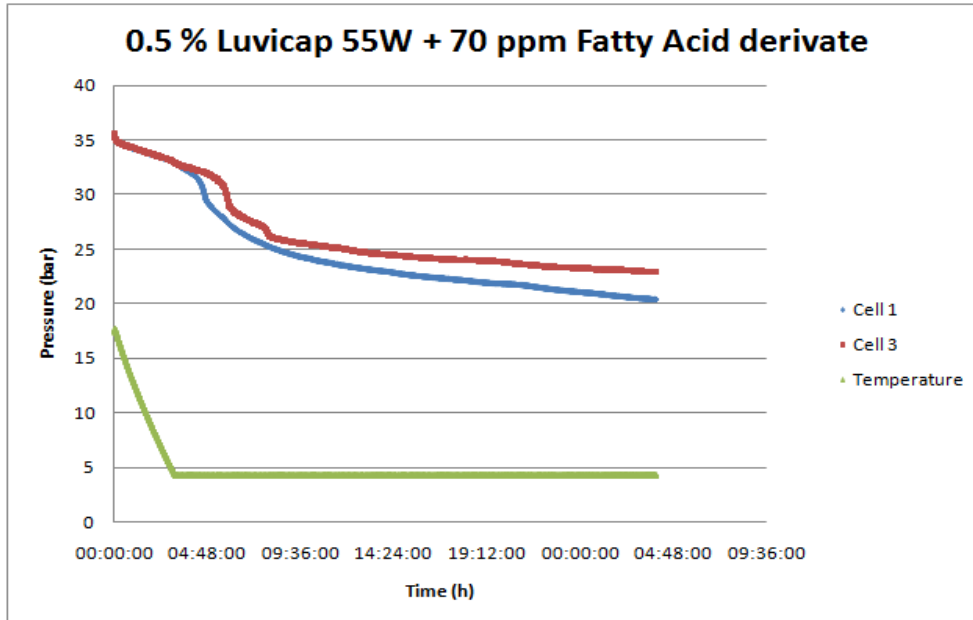


Figure 54 Performance of Luvicap 55W in presence of 70 ppm fatty acid derivate

Induction time for each test were found (table 14). Percent reduction was calculated based on the minimum induction time 19.5 h which represent 100 %.

Table 14 Induction time for all test mixtures

Test mixtures	Induction time (h)	Induction time (h)	Performance of KHI
0.5 % Luvicap 55W	19.5	28	100 %
30 ppm Imidazoline A	8.5	13.5	44
80 ppm Imidazoline A	6.5	7.5	33
25 ppm Imidazoline B	8	13.5	41
50 ppm Imidazoline B	4.5	6	23
20 ppm Fatty Acid derivate	17	25	87
70 ppm Fatty Acid derivate	8.5	9.5	44

Minimum induction time for each mixture is presented graphically in figure 55.

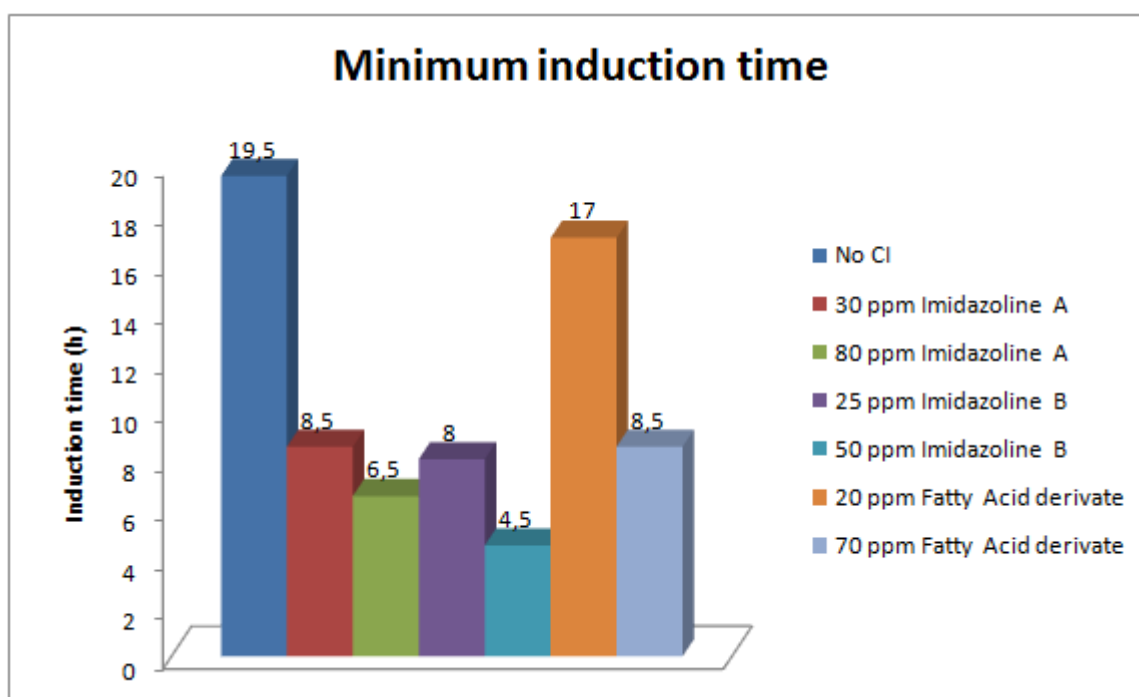


Figure 55 Induction time for each test with and without CIs in solution

Minimum induction time of Luvicap 55W with no CI present (19.5 h) was set as a baseline of 100 %. Figure 56 show the percent performance of each mixture.

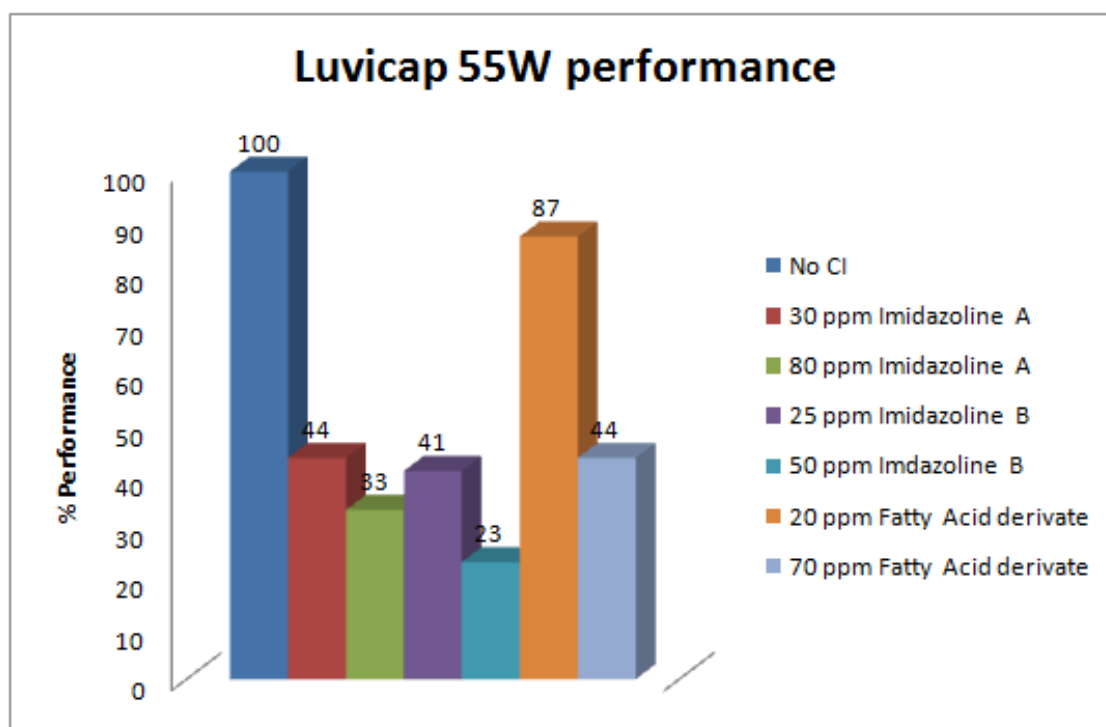


Figure 56 Percent performance of Luvicap 55W in presence of CIs

4.3.4.1 Summary

It was clearly an interaction between the KHI and the CIs after evaluating the various induction times. Induction time was reduced with more than 50 % in all of the mixtures except for the fatty acid derivate added at CMC (20 ppm). Luvicap 55W was only reduced with 13 % in presence of 20 ppm fatty acid derivate.

Higher CI concentration resulted in a higher degree of KHI reduction.

Table 15 summarizes the main results from the corrosion and hydrate tests.

Table 15 Summary of results

CI	Corrosion test	Hydrate test	Compatibility
Imidazoline A	<ul style="list-style-type: none"> • Foaming problems Reduction of CI performance: <ul style="list-style-type: none"> • At CMC: 55% • Above CMC: 11% • Moderate impact of KHI 	Induction time reduction: <ul style="list-style-type: none"> • At CMC: 56 % • Above CMC: 67% 	Not compatible
Imidazoline B	<ul style="list-style-type: none"> • Foaming problems Reduction of CI performance: <ul style="list-style-type: none"> • At CMC: 12% • Above CMC: 1% • Minimal impact of KHI 	Induction time reduction: <ul style="list-style-type: none"> • At CMC: 59 % • Above CMC: 77% 	Not compatible
Fatty acid derivate	Increased CI performance: <ul style="list-style-type: none"> • At CMC: 3% • Above CMC: 2% • Low impact of KHI 	Induction time reduction: <ul style="list-style-type: none"> • At CMC: 13 % • Above CMC: 56% 	Moderately compatible

5 CONCLUSION

Corrosion tests and hydrate tests were performed to investigate possible interactions between a KHI and different CIs. Although reproducibility in the corrosion tests was fairly poor some trends were seen. These are as follows:

- Luvicap 55W impacted the performance of Imidazoline A and Imidazoline B negatively. Imidazoline A performance was reduced with 55 % (at CMC) and 11 % (above CMC). Imidazoline B performance was reduced with 12 % (at CMC) and 1 % (above CMC). Fatty acid derivate efficiency was on contrary increased with 3 % (at CMC) and 2 % (above CMC).
- Imidazoline B performed better than Imidazoline A in presence of Luvicap 55W.
- Corrosion test results were more consistent when CI was added above CMC than below. This emphasized the importance of finding the CMC for a surfactant solution, prior the CI testing.
- All CI's had a negative effect on Luvicap 55W. The KHI performance was reduced with more than 50 % in most of the tests. An exception was the fatty acid derivate (at CMC) which reduced the KHI performance with 13 %.
- One CI/KHI combination showed moderately compatibility in both of the tests; fatty acid derivate and Luvicap 55W.

6 RECOMMENDATIONS

This study revealed both negative and positive interactions between the CIs and the KHI. In order to find a compatible CI/KHI package with the chosen chemicals, more research is required. Some suggestions have been summarized. These are as follows:

- Add a defoamer or change the setup in the corrosion tests to decrease foaming and chemical loss.
- Continue this study by carry out more hydrate tests with the best CI candidate (fatty acid derivate) with increased amount of Luvicap 55W at 32 bars in order to compare the results.
- Perform more replicates for both corrosion and hydrate tests to validate the results in a thorough statistical approach.
- Study the degree of interaction by varying the CI and KHI concentration at a constant pressure. Suggested test concentrations are summarized in table 16. Holding the concentration ratio constant between the CMC and above could be beneficial for comparison results.

Table 16 Suggestion of test concentrations

[CI]	[KHI]
CMC	0.5 %
2x CMC	1.0 %
3x CMC	1.5 %

- Try to fully understand the interactions between the CI/KHI:
 - Observe surface interaction by measuring surface tension for different mixtures.
 - Investigate chemical interaction at a molecular level by analyzing the combined molecules with LC/MS.
- Investigate interaction in a system varying different parameters such as: pH, brine concentration and pressure.
- In the search of finding a proper CI/KHI package, other classes of CIs could be tested in presence of Luvicap 55W.

7 REFERENCES

1. Read, P.A. and B. Neigart, *Kjemikalier*, e.-. petroleum, Editor 2002, Vett & Viten.
2. Pakulski, M.K., *Accelerating Effect of Surfactants on Gas Hydrates Formation*, in *International Symposium on Oilfield Chemistry*2007: Houston, Texas, U.S.A.
3. Chilingarian, G.V., R. Mourhatch, and G.D. Al-Qahtani, *The Fundamentals of corrosion and scaling for petroleum and environmental engineers*2008, Houston, Tex.: Gulf Publishing Co. xviii, 276 s.
4. Chemicals, M.-I.P., *Product Catalog*, A.S.C. M-I SWACO, Editor: Sandnes.
5. Byars, H.G., *Corrosion control in petroleum production*. TPC publication. Vol. 5. 1999, Houston: NACE. XIII, 309 s.
6. Kelland, M.A., *Production chemicals for the oil and gas industry*2009, Boca Raton, Fla.: CRC Press. XVII, 437 s.
7. Kermani, M.B. and A. Morshed, *Carbon Dioxide Corrosion in Oil and Gas Production A Compendium*. Corrosion, 2003. **59**(08).
8. Ahmad, Z., *Principles of corrosion engineering and corrosion control*2006, Boston, MA: Elsevier/BH. xv, 656 s.
9. Fink, J.K., *Oil field chemicals*2003, Amsterdam: Gulf Professional Publ. X, 495 s.
10. Hedges, W., J.L. Dawson, and J.W. Palmer, *A working party report on the use of corrosion inhibitors in oil and gas production*. Publications. Vol. no 39. 2004, London: Institute of Materials. xiv, 106 s.
11. CAPROCO, *Linear Polarization Resistance (LPR), General Information*, 2011, CAPROCO.
12. Myers, D., *Surfaces, interfaces, and colloids: principles and applications*1999, New York: Wiley. xx, 501 s.
13. Schramm, L.L., *Surfactants: fundamentals and applications in the petroleum industry*2000, Cambridge: Cambridge University Press. viii, 621 s.
14. Attension. *Surface Tension*. 2011; Available from: <http://www.attension.com/surface-tension.aspx>.
15. Farn, R.J., *Chemistry and Technology of Surfactants*2006: Wiley-Blackwell. 336.
16. Chemistry, R.S.o. *Ink Chemistry*. 2011 24.03.2011]; Available from: <http://www.rsc.org/chemistryworld/issues/2003/March/inkchemistry.asp>.
17. KRUSS, G. *KRUSS Advancing Surface Science: K6- Educational Tensiometer*. 2011; Available from: <http://www.kruss.de/en/home.html>.
18. Sloan, E.D. and C.A. Koh, *Clathrate hydrates of natural gases*2008, Boca Raton, Fla.: CRC Press. XXV, 721 s., pl.
19. Carroll, J.J., *Natural gas hydrates: a guide for engineers*2009, Amsterdam: Elsevier. XVII, 276 s.
20. Peytavy, J.-L., P. Glenat, and P. BOURG, *Kinetic Hydrate Inhibitors - Sensitivity towards Pressure and Corrosion Inhibitors*, in *International Petroleum Technology Conference*2007: Dubai, U.A.E.
21. Blog, M.T. *Hydrates-a Novel Concept for Plugging Deep-Sea Severed Pipeline*. 2010, May 22; Available from: <http://mikstechnology.wordpress.com/2010/05/22/hydrates-a-novel-concept-for-plugging-deep-sea-severed-pipeline-proposed-scenario-for-bp-gulf-of-mexico-spill/>.
22. Sloan, E.D., *Fundamental principles and applications of natural gas hydrates*. Nature, 2003. **426**(6964): p. 353-363.
23. Engineering, H.W.I.o.P. *Centre for Gas Hydrate Research*. 2011; Available from: http://www.pet.hw.ac.uk/research/hydrate/hydrates_what.cfm.
24. Kelland, M.A., *History of the Development of Low Dosage Hydrate Inhibitors*. Energy & Fuels, 2006. **20**(3): p. 825-847.

25. Sloan, E.D., *Natural gas hydrates in flow assurance* 2011, Amsterdam: Elsevier. XXII, 200 s.
26. Production, E.a. *Supercharged methanol cuts hydrates*. 2007, April; Available from: <http://www.epmag.com/archives/features/350.htm>.
27. Kelland, M.A., T.M. Svartaas, and L.A. Dybvik, *Control of Hydrate Formation by Surfactants and Polymers*, in *SPE Annual Technical Conference and Exhibition* 1994: New Orleans, Louisiana.
28. Kelland, M.A., T.M. Svartaas, and L. Dybvik, *A New Generation of Gas Hydrate Inhibitors*, in *SPE Annual Technical Conference and Exhibition* 1995: Dallas, Texas.
29. MacDonald, A., et al., *Field Application of Combined Kinetic Hydrate and Corrosion Inhibitors in the Southern North Sea: Case Histories*, in *SPE Gas Technology Symposium* 2006: Calgary, Alberta, Canada.
30. Fu, B., *Development Of Non-Interfering Corrosion Inhibitors For Sour Gas Pipelines With Co-Injection Of Kinetic Hydrate Inhibitors*, in *CORROSION 2007* 2007, NACE International: Nashville, Tennessee.
31. J.J. Moloney, W.Y. Mok, and C.G. Gamble, *Compatible Corrosion And Kinetic Hydrate Inhibitors For Wet Sour Gas Transmission Lines*, in *CORROSION 2009* 2009, NACE International: Atlanta, GA.
32. Fu, S.B., L.M. Cenegy, and C.S. Neff, *A Summary of Successful Field Applications of A Kinetic Hydrate Inhibitor*, in *SPE International Symposium on Oilfield Chemistry* 2001: Houston, Texas.
33. Kalogerakis, N., et al., *Effect of Surfactants on Hydrate Formation Kinetics*, in *SPE International Symposium on Oilfield Chemistry* 1993: New Orleans, Louisiana.
34. Ramaswamy, D. and M.M. Sharma, *The Effect of Surfactants on the Kinetics of Hydrate Formation*, in *SPE International Symposium on Oilfield Chemistry* 2011: The Woodlands, Texas, USA.
35. UiS, *Biophysical Chemistry course literature: Surface Tension*, 2008.
36. Villano, L.D., et al., *A Study of the Kinetic Hydrate Inhibitor Performance and Seawater Biodegradability of a Series of Poly(2-alkyl-2-oxazoline)s*. *Energy & Fuels*, 2009. **23**(7): p. 3665-3673.
37. Hansson, P. and B. Lindman, *Surfactant-polymer interactions*. *Current Opinion in Colloid & Interface Science*, 1996. **1**(5): p. 604-613.

8 LIST OF APPENDIX

1. Appendix 1: M-I SWACOs Bubble Test Standard
2. Appendix 2: Phase envelope for gas mixture G11 in 0.1 wt% NaCl



Test Method **Standard Bubble Test**

Site **Aberdeen**

Reference **PT-TM-0065**

1 Introduction

1.1 Purpose

The bubble (or kettle) test is a widely used and accepted test method for the evaluation of oil field corrosion inhibitors. It is based on the principle of linear polarization resistance (LPR). In essence, the test involves an electrochemical evaluation of inhibitor performance in a vessel of fluids which is constantly being sparged with corrosive gas – normally CO₂ (hence ‘bubble test’). This test is ideal for rapidly carrying out a large number of tests, for example as the first stage of corrosion inhibitor selection, or for screening a wide range of field conditions.

It is convenient to use a gantry of cells connected to an automated corrosion rate measuring system.

The performance of corrosion inhibitors can be evaluated with respect to corrosion protection performance and oil/water partitioning ability. Field conditions can be simulated as closely as possible using natural or synthetic brines and crude oils.

1.2 Method Scope, Inputs and Limitations

This test method is based on reference ASTM G59 (“Practise for Conductivity, Potentiodynamic Polarization Resistance Measurements”)

Tests can only be carried out at ambient pressure, and at temperatures not exceeding 90°C. Tests may be performed using just an aqueous phase in the cell, or a mixture of aqueous and oil phases (using kerosene or field crude). However, water cut must typically be at least 20% to give a stable reading. Typically the test is run with CO₂ sparging to remove oxygen from the system to simulate e.g. pipeline conditions. However, this may be omitted if the corrosion rate in an oxygenated environment (e.g. a chemical storage tank) is being investigated.

Results may be reported in either mm/year or milli-inches/year (mpy) and should be quoted to two decimal places.

1.3 Health, Safety and Environmental

This test method has been prepared in accordance with the precautions outlined in Risk Assessment RA-063. This should be read prior to performing the test and all precautions followed.

- Make sure all leads and pipe work are tidy and do not come into contact with hot surfaces.
- Check the supply of carbon dioxide prior to and after screening, in order to reduce the risk of the gas running out either during or after the LPR screening and thus allowing oxygen ingress.
- Ensure leads are not loosely connected, in case they are displaced during screening.
- Make sure water is running through the condensers when high temperatures are been used, and also check for leaks.

The MSDS for all chemicals used for this test method must be consulted and suitable precautions taken, with a COSHH assessment being performed if required.

2 Equipment and Maintenance

The following test equipment is required

- Bubble test apparatus
- Includes : Hot plate/Stirrer,
- Magnetic stirring bar,
- Glass corrosion cells, lids and stopper.
- Metal clamps for lids
- Gas sparge tubes linked to CO2 supply,
- Condensers,
- Electrodes attached to ACM instruments PC monitoring system,
- PC for logging.
- Micro Pipette
- Silicon carbide paper

REAGENTS

- Test brine
- Odourless kerosene (if generic oil phase required)
- Field Crude (if specific oil phase required and only if ventilation allows)
- Corrosion inhibitor
- Acetone
- ~5% Hydrochloric acid solution

3 Method

Vessel Cleaning

Baseline corrosion values in brine can be affected by tiny amounts (<1ppm) of certain corrosion inhibitors. Therefore it is essential to thoroughly cleanse the glassware before each test as follows

1. Rinse vessel and underside of lid with deionised water.
2. Fill the vessel with a 5% HCl solution and allow to soak for a few hours if required.
3. Thoroughly rinse with tap water followed with de-ionised water.
4. Rinse with acetone if required for drying.
5. Take care to rinse the inside of the gas sparging and probe entry tubes.
6. Finally, wipe the exterior surfaces of the glassware dry with tissue but do not apply to internal surfaces.

Conditioning of Solution

1. The brine is prepared without the bicarbonate (if applicable) the bicarbonate in the test brine is added at a later stage.
2. Pour the brine (1Litre if not using an oil phase, if using oil the total volume of oil and water should be 1L) into the vessel then clamp the lid in place. If using oil in the tests, do not add oil until probe is in the brine (step 3.5).
3. Attach the condenser in to one of the non-vertical probe entry ports and turn on water supply. Insert the gas sparge tube in to the small vertical probe entry port add the thermocouple to the other non vertical entry port and place the glass stopper in to the large centre entry port.
4. Start the magnetic stirrer (ca 300rpm). The stirring speed in the test can influence the corrosion rate. Baseline rates increase by ca 30% as the speed is raised from 0 to 100 rpm, above this there is little influence of stirring on corrosion rate. Operating at 300 rpm, as specified here, ensures that slight differences in stirring have negligible effect. Set the heating controller to the desired temperature and switch on.
5. Deaerate with CO₂ for 2 hours to remove oxygen from the system. Flow meters should be set at 500ml/min. Any bicarbonate required can be added after brine has been purged with CO₂ for 2 hours, but should be added as a solution in deionised water.

Electrode Preparation

Three element linear polarisation resistance (LPR) probes containing mild steel test electrodes measure corrosion rates. The preparation of the electrodes is one of the key parameters in running a meaningful test. New electrodes should be used in each test and cleaned prior to use. Always use disposable gloves to handle the electrodes.

1. Rinse the probe body several times with deionised water.
2. Vigorously scrub all surfaces, including the screw threads on the bottom of the probe.
3. Rinse twice with deionised water.
4. Rinse with Acetone.

The electrodes are shipped inside a paper envelope, which is impregnated with a vapour phase corrosion inhibitor (i.e. VCI paper). It is recommended that the electrodes be cleaned with 1200 grit SiC abrasive paper wetted with deionised water, and then dried with Acetone.

SiC paper scours the entire metal surface producing an appearance of fine scratches all over.

Following the Acetone rinse allow to dry and use immediately.

Corrosion Monitoring, PC Set-Up

ACM Bubble Test Software

1. Log in to the computer with MI username and password as usual.
2. The corrosion monitoring software is selected by double clicking on the Gill 12 Serial No. 456 – Sequencer icon on the desktop.
3. The 12 channel tabs across the top refer to each of the 12 leads available. Select the channel that corresponds to the lead you are using.
4. The usual software set up has the name long term [99999 measurements] in the top of the sequencer list on the left hand side of the window. Underneath this there is long term – LPR corrosion rate sweep.
5. Double clicking on Long term [99999 measurements] opens a window that allows the frequency and amount of measurements to be altered if required. As the logging can be stopped when sufficient data is collected there is no need to select the exact number of readings you need. The usual time delay between readings is 10 minutes but this can be changed if desired.
6. Double clicking on Long Term – LPR corrosion rate sweep opens a window. The standard settings are as follows. Start potential = -10mV, End potential = 10, Sweep rate = 20mV/min, Ba = 113mV, Bc=113mV, readings per test = Automatic, offset rest potential is selected, start of test cell settle time = 30seconds, internal counter resistor – auto-ranging during test is selected at start of test = auto.
7. In the bottom section of the window the settings are as follows. Configured as = normal. Area = 4.700E+00 (For standard bubble test. For RCE this will be 3.000E+00). Metal = mild steel. Data storage – insert the file name of the folder where you would like the data stored. The computer is networked so the data can be stored on the L drive or computers own C drive.
8. Once the filename and LPR set up is confirmed the test is started by first clicking on the globe icon entitled Core Run on the right hand side. A window asking if changes to the core should be updated will appear. To ensure the correct file location the update should be allowed for all channels you need to use.
9. In core running all channels will open windows. A channel control window will open. To start a test click enabled on the channel or channels corresponding to your test.

10. Click on the channel No. on the top tool bar to bring up a graph of the test. During the test long term corrosion rate graph or short term current/potential graphs can be viewed by clicking on the icon of a graph on the top left of the channel window.
11. To end the test, click the Dis button on the tool bar of the channel graph or click on the disabled button in the channel control window.

Inserting the Electrode into the Cell

1. Remove the large glass stopper from the vessel, and carefully lower the probe into the solution. The counter current of CO₂ will prevent any ingress of oxygen.
2. If using oil, add to the surface of brine after electrode is inserted.
3. Attach the probe to the corrosion monitoring equipment and trigger logging on PC by clicking enable all in the Group control window.
4. Inhibitor should be added after establishing a stable baseline corrosion rate for 1-2 hours. Add the inhibitor by removing the temperature probe and injecting the desired concentration in to the fluid through this port.
5. Replace temperature probe as soon as possible to prevent overheating of the fluid.

Results and Calculations

At the end of the test, the CO₂ and hot plates should be turned off, probes removed and test equipment cleaned as outlined above.

1. If test has not finished and you wish to end the test in the group control window select "disable all"
2. To retrieve the results go to start menu, programs, ACM instrument Version 5, Analysis.
3. In the Analysis window move cursor over the list of files on the right hand side to expand.
4. The most recent tests will be displayed at the top.
5. Select the file you want, click on the long term tab, click on the graph and drag down to the data bank table at the bottom.
6. Select all the files you wish to compare together. Select the graph icon at the top.
7. Once graph is displayed click on the graph drop down menu and click on Mils/year vs time.
8. Once new graph is displayed go to edit and select copy as and tab separated text.
9. Open an Excel spread sheet and paste the data.
10. Use Excel template to plot the desired graphs for a report.

The efficiency of the inhibitor is calculated as follows:

$$\% \text{ Eff} = \frac{(C1 - C2)}{C1} * 100$$

C1 = Uninhibited corrosion rate (blank)

C2 = Inhibited corrosion rate (at 15 hours)

APPENDIX 2- HYDRATE PHASE ENVELOPE FOR GAS MIXTURE IN 0.1 % NaCl

